A THESIS SUBMITTED TO
THE GRADUATE SCHOOL OF NATURAL AND APPLIED SCIENCES
OF ÇANKIRI KARATEKİN UNIVERSITY

STUDY AND IMPROVE THE PERFORMANCE OF MULTIUSER SHARING ACCESS FOR 5G NETWORKS

IN PARTIAL FULFILLMENT OF THE REQUIREMENTS
FOR
THE DEGREE OF MASTER OF SCIENCE
IN
ELECTRICAL AND ELECTRONICS ENGINEERING

BY

WAEL SADEQ ABD ALI FANHARAWY

ÇANKIRI

2023

STUDY AND IMPROVE THE PERFORMANCE OF MULTIUSER SHARING ACCESS FOR 5G NETWORKS

By Wael Sadeq Abd Ali FANHARAWY

June 2023

We certify that we have read this thesis and that in our opinion it is fully adequate, in scope and in quality, as a thesis for the degree of Master of Science

Advisor **:** Prof. Dr. Murat ARI

Examining Committee Members:

Chairman **:** Prof. Dr. Murat ARI
Electrical and Electronics Engineering
Çankırı Karatekin University

Member **:** Prof. Dr. M. Cengiz TAPLAMACIOĞLU
Electrical and Electronics Engineering
Gazi University

Member **:** Assoc. Prof. Dr. Fatih KORKMAZ
Electrical and Electronics Engineering
Çankırı Karatekin University

Approved for the Graduate School of Natural and Applied Sciences

Prof. Dr. Hamit ALYAR
Director of Graduate School

I hereby declare that all information in this document has been obtained and presented in accordance with academic rules and ethical conduct. I also declare that, as required by these rules and conduct, I have fully cited and referenced all material and results that are not original to this work.

Wael Sadeq Abd Ali FANHARAWY

ABSTRACT

STUDY AND IMPROVE THE PERFORMANCE OF MULTIUSER SHARING ACCESS FOR 5G NETWORKS

Wael Sadeq Abd Ali FANHARAWY

Master of Science in Electrical and Electronics Engineering

Advisor: Prof. Dr. Murat ARI

June 2023

Non-orthogonal Multiple Access (NOMA) technologies are considered as one of the proposed solutions to meet the requirements of the fifth generation. It has the ability to improve spectral efficiency through users' sharing of radio resources, and increasing the degree of freedom in the number of non-orthogonal resources. However, these technologies suffer from interference between users' signals due to the absence of orthogonality, which can be reduced by using advanced receivers of high complexity. The Power Domain non-orthogonal multiple access (PD-NOMA) and Multi-User Sharing Access (MUSA) schemes are types of NOMA Technologies. They improve system efficiency by increasing the number of users on the same radio resource and achieving higher flexibility in reuse of system resources. Both schemes can be used in both downlink and uplink systems based on Minimum Mean Square Error - Successive Interference Cancellation (MMSE-SIC) receiver to improve decoding performance. In this study, the performance of the MUSA system has been improved in the uplink by applying the PD-NOMA scheme and the effect on the error probability and minimum rate performance of the system caused by cross-correlation between the complex spreading sequences and the power allocation scheme has been analyzed. Also, the optimal solution for the spreading sequences and the power coefficients allocation that achieve the maximum minimum signal to interference and noise ratio on which the rate and bit error rate performances in the hybrid NOMA scheme depends, has been studied. Two iterative algorithm has been proposed to solve the optimization problem separately. OMA (Orthogonal Multiple Access) scheme has been proposed as a benchmark. The simulation results showed that our proposed scheme outperforms on the OMA benchmark in terms of achievable minimum rate per user and total power consumption. Besides, the bit error rate performance is improved in the proposed scheme compared to the conventional MUSA scheme.

2023, 62 pages

Keywords: Orthogonal multiple access, Multi-user share access, Minimum mean squared error, Power field non-orthogonal multiple access, Non-orthogonal multiple access, Sequential interference cancellation

ÖZET

5G AĞLARI İÇİN ÇOK KULLANICI PAYLAŞIM ERİŞİMİNİN PERFORMANSINI ARAŞTIRIN VE GELİŞTİRİN

Wael Sadeq Abd Ali FANHARAWY
Elektrik ve Elektronik Mühendisliği, Yüksek Lisans
Tez Danışmanı: Prof. Dr. Murat ARI
Haziran 2023

Ortogonal Olmayan Çoklu Erişim (NOMA) teknolojileri, beşinci neslin gereksinimlerini karşılamak için önerilen çözümlerden biridir. Kullanıcıların radyo kaynaklarını paylaşması ve ortogonal olmayan kaynakların sayısındaki serbestlik derecesini artırması yoluyla spektral verimliliği artırma yeteneğine sahiptir. Bununla birlikte bu teknolojiler, ortogonalitenin olmaması nedeniyle kullanıcıların sinyalleri arasındaki, yüksek karmaşıklığa sahip gelişmiş alıcılar kullanılarak azaltılabilen, girişime maruz kalmaktadır. Güç domeni ortogonal olmayan çoklu erişim (PD-NOMA) ve Çoklu Kullanıcı Paylaşım Erişimi (MUSA) şemaları; aynı radyo kaynağındaki kullanıcı sayısını artırarak ve sistem kaynaklarının yeniden kullanımında daha fazla esneklik sağlayarak, sistem verimini iyileştiren NOMA teknolojileri türleridir. Her iki şema da kod çözme performansını artırmak için Minimum Ortalama Karesel Hata - Ardışık Girişim İptali (MMSE-SIC) alıcısına dayalı hem aşağı bağlantı (uplink) hem de yukarı bağlantı (downlink) sistemlerinde kullanılabilirler. Bu çalışmada, PD-NOMA şeması uygulanarak MUSA sisteminin yukarı bağlantı hattındaki performansı iyileştirilmeye çalışılmıştır. Karmaşık yayılma dizileri ile güç tahsis şemasının çapraz korelasyonu nedeniyle sistemin hata olasılığına ve minimum oran performansına olan etkisi etkisi araştırılmıştır. Ayrıca, hibrit NOMA şemasındaki hız ve bit hata oranı performanslarının bağlı olduğu maksimum-minimum sinyal-girişim ve gürültü oranını elde eden yayılma dizileri ve güç katsayıları tahsisi için en uygun çözüm elde edilmeye çalışılmıştır. Optimizasyon problemini ayrı ayrı çözmek için iki yinelemeli algoritma önerilmiştir. Ayrıca, karşılaştırma amacıyla Ortogonal Çoklu Erişim (OMA) şeması önerilmiştir. Simülasyon sonuçları önerilen yöntemin, kullanıcı başına elde edilebilir minimum oran ve toplam güç tüketimi açısından OMA kıyaslamasında daha iyi performans verdiğini göstermiştir. Ayrıca önerilen şemada bit hata oranı performansı geleneksel MUSA şemasına göre iyileştirilmiştir.

2023, 62 sayfa

Anahtar Kelimeler: Ortogonal çoklu erişim, çoklu kullanıcı paylaşım erişimi, Minimum ortalama karesel hata, Power domain ortogonal olmayan çoklu erişim, Ortogonal olmayan çoklu erişim, Ardışık girişim iptali

PREFACE AND ACKNOWLEDGEMENTS

I would like to thank my thesis advisor, Prof. Dr. Murat ARI, and Researcher assistant Mahmud Esad YİĞİT for thier patience, guidance and understanding.

Wael Sadeq Abd Ali FANHARAWY
Çankırı-2023

CONTENTS

LIST OF ABBREVIATIONS

AWGN	Additive white gaussian noise
BER	Bit error rate
EE	Energy efficiency
FDMA	Frequency division multiple access
FDD	Frequency domain division
LTE	Long term evolution
LTEA	Long term evolution advanced
MMTC	Massive machine type communication
MM-Wave	Millimeter waves
MMSE	Minimum mean square error
MMSE-SIC	Minimum mean square error - successive interference cancellation
MIMO	Multipule input multipule output
MUD	Multi-user detection
MUSA	Multi-user shared access
NOMA	Non-orthogonal multiple access
OFDMA	Orthogonal frequency division multiple access
OMA	Orthogonal multiple access
PIC	Parallel interference cancelation
PDMA	Pattern division multiple access
PAPR	Peak-to-average-power ratio
PSK	Phase shift keying
PD-NOMA	Power domain non-orthogonal multiple access
QAM	Quadrature amplitude modulation
SINR	Signal-to-interference-and-noise ratio
SNR	Signal-to-noise ratio
SC-FDMA	Single carrier-frequency division multiple access
SCMA	Sparse code multiple access
SE	Spectral efficiency
SIC	Successive interference cancellation
SC	Superposition coding
TDMA	Time division multiple access
TDD	Timedomain division
URLLC	Ultra reliable low latency communication
UOL	User overloading
ZF	Zero forcing

LIST OF FIGURES

LIST OF TABLES

1. INTRODUCTION

Development of cellular systems began in the eighties of the last century after Maxwell Games Clark Maxwell discovered the electromagnetic waves that can propagate at a speed close to the light speed, and then Heinrich Hertz succeed in generating and detecting these waves, which were called later radio waves, so the first generation (1G) of cellular systems appeared. Successively the subsequent generations appeared at a rate of every ten years until the fifth generation as a result of the large increasing spread of the applications of these systems (Paudel 2018).

Cellular communication systems have been developed through successive generations, the first-generation analog 1G for voice calls, then second-generation (2G) in the 1990s, and the third generation (3G) at the beginning of the current century, and ending to the fourth generation (4G) in 2010. With the rapid technological development in various fields, many new applications appear such as Internet of Things applications. The work for the fifth generation of cellular communication systems began by looking for advanced technologies or developing current techniques to keep up with new requirements and become able to improve various performance standards as spectral effectiveness, the number of users, and time-response latency (Salih 2020).

Multiple access is considered as the basic technology that allows the wireless base station to deal and provide services to a large number of users or devices at the same time. Previous generations of cellular systems depended on the Orthogonal Multiple Access (OMA), which uses the orthogonal resource elements of the system, to enable user access to the network. One or more orthogonal resource elements are allocated for every user such as using Orthogonal Frequency Division Multiple Access (OFDMA), that every user uses different carrier frequencies. Figure 1.1 shows some multiple access techniques were adopted according to the resource allocation manner to address new challenges in every generation. While Non-Orthogonal Multiple Access (NOMA) depends on Superposition Coding (SC) technique for transmitted signals in power or code domain at the transmitter side, and Interference Cancellation (IC) schemes are used at the receiver side. The NOMA schemes are considered as a promising technique of radio access techniques to improve performance in generations of cellular communications, especially with the limited radio resources such as a limited radio spectrum (Budhiraja 2021).

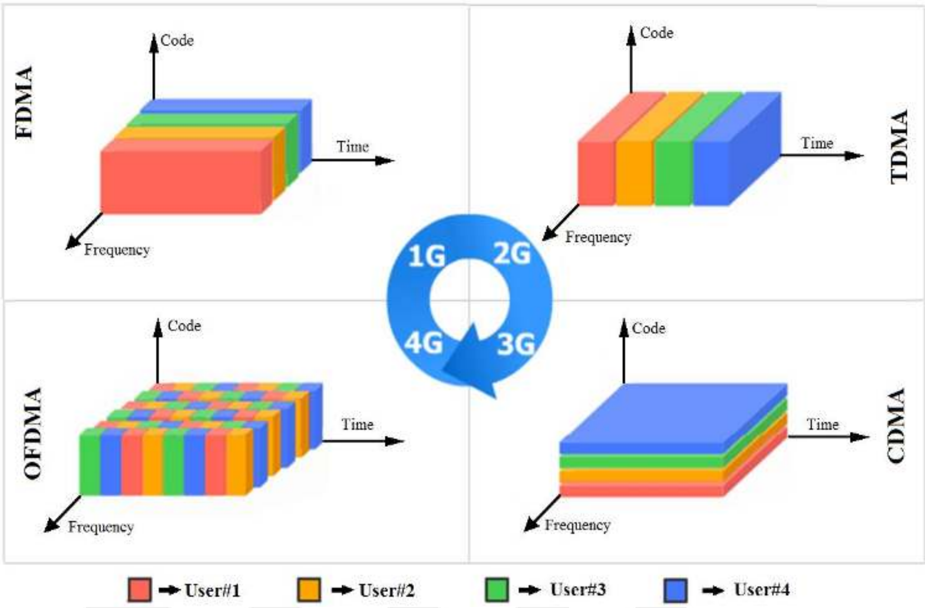

Figure 1.1 Multiple accesses for current generations (Budhiraja 2021)

OMA technologies have achieved good performance for the applications and services provided by previous generations. In addition, it is characterized by simplicity compared to NOMA technologies. Because of the critical requirements such as the IoT and the limited orthogonal resources, OMA technologies became unable to meet the large increasing requirements of wireless communication systems, (Vaezi 2018).

1.1 Thesis Objective

The thesis aims to improve the performance of Multi-user Shared Access (MUSA), which is a scheme of the NOMA for uplink\downlink transmission. The performance of the MUSA scheme are evaluated for a high number of users (high user overload) in the NOMA uplink, then the Power Domain NOMA (PD-NOMA) scheme is applied.

Firstly, it is necessary to study the concepts of non-orthogonal multiple access with its various schemesespecially the MUSA and PD-NOMA schemes. The effect on the bit error rate (BER) and rate performance of the system have to be studied as long as it is caused by cross-correlation between the complex spreading sequences and the power allocation scheme. The study includes also the separate search for the optimal solution for the spreading sequences and the power coefficients that achieve the maximum minimum signal to interference and noise ratio within the limits of the maximum power and the required minimum rates for each user. Finally, the comparsion study with the OMA is included, and the impact of the proposed method on the performance is discussed.

1.2 Importance of the Thesis

OMA technologies are simple compared to NOMA technologies, which increase the complexity of the receiver because of the high complexity algorithms needed to eliminate the interference between the interfering signals. On the other hand, NOMA technologies can achieve many advantages over OMA technologies in different performance criteria, such as:

- Increasing the spectral efficiency (SE) through users sharing radio resources.
- Supporting a large number of connections by increasing the degree of freedom in the number of non-orthogonal resources.
- Reducing the latency by reducing signaling and enabling grant-free transmissions.
- Greater fairness is achieved by allocating more power to the user with low channel gain.
- Compatibility with OMA, and advanced technologies such as massive multipule input multipule output (MIMO).

This thesis's importance comes from consideration that NOMA is one of the solutions for the increasing requirements in the expected scenarios of the fifth-generation communication system. One of the NOMA scheme types is called MUSA, which simplifies the access procedure significantly by adopting a grant-free access strategy.

2. LITERATURE REVIEW

The non orthogonal multiple access is proposed for 5G to improve system performances, and it is expected to extend up to the next generation due to its compatibility with the advanced emerging technologies (TATARIA 2021). However, some issues and challenges in NOMA systems are still an open problems such as interference management, high computational complexity, practical implementation, and error propagation. To address that challenges, it is necessary to develop new multiple access techniques and find solutions for NOMA (Alsabah 2021).

Dai *et al.* (2018) discussed the principles and concepts of NOMA technologies and the most important advantages that can be achieved using these technologies. The results show that the total user rate can be improved by using PD NOMA compared to OFDMA scheme, also the SCMA performance outperforms Long term evolution (LTE) system in terms of throughput.

According to the SC domain, NOMA schemes can be divided into two parts: power domain NOMA and code domain NOMA. Some of the researches and challenges were presented about these systems, where most important is to improve the desired performance standards and address the impact of the error propagation, increasing as the user overloading (UOL) increases in the network. Both latency and SE performances can be improved based on NOMA in various senarios and applications such as vehicle to everything communication, millimeter wave and MIMO systems. (Budhiraja 2021).

NOMA's uplink technologies wre categorized depending on the nature of the transmitter use of radio resources such as using short or long spreading sequences, scrambling, and interleaving. The MUSA scheme utilizes short spreading sequences, while multi dimensions constellation based on codebooks are used for PDMA and SCMA schemes (Shan 2017).

The conventional power domain NOMA technique decreases the outage probability and increases the achievable rate compared to the conventional OMA systems. Also the outages and rate performances of the cooperative NOMA systems outperforms to the cooperative OMA systems. Another benefit of PD-NOMA represented in its compatibility with advanced technologies such as massive MIMO communication, (Islam 2017).

However, higher capacity regions in downlink and uplink PD-NOMA can be acheived compared to OMA by assigning suitable transmitted powers. Average user throughput gain, specially the cell-edge users, can be improved based on PD-NOMA technique where the allocated transmission powers are controlled carefully (Higuchi 2015).

Power efficiency in both PD-NOMA and OFDMA system increases as SE increases for lower data rate requirements, while for higher rate requirements the power efficiency decreased. Moreover, higher SE and power efficiency can be achieved in PD NOMA compared to OFDMA. Error probability performance in SCMA system is better than PD-NOMA system, which outperforms in terms of the total rate specially for large number of users (Shah 2021).

The performance of the MUSA scheme was compared to SCMA and PDMA techniques in terms of BER for uplink transmission, where the SCMA scheme outperforms MUSA and PDMA at low UOL but with increased user overload, MUSA outperforms SCMA. The real and imaginary parts for each complex element of spreading sequence belong to a set of five real elments (Eid 2019).

NOMA technologies have the feature of compatibility with OMA technologies and the advanced technologies proposed for fifth-generation systems such as massive MIMO, as it contributes to increasing the throughput of these systems. The sum rate in OMA system can be improved by 9% when NOMA technique is used instead of it (Liu *et. al* 2017).

On the other hand, cognitive radio systems can be used with multiple antennas systems,as long as it is considered as a special case of NOMA to improve the SE within the limited radio resources (Bhatia 2018).

The performance of the MUSA scheme was evaluated based on three ordered methods at UOL=150% in the Rayleigh fading channel. In the first method, the signal to interference and noise ratios are utilized to reordering the users. The second method depends on the signal to noise ratios, while the third calculates the column norm of system matrix. The results show that the first method outperformed compared to the second and third in terms of BER (Id 2017).

The MUSA technique also achieves better throughput compared to SCMA and OFDMA in the additive white Gaussian noise (AWGN) channel at a high signal to noise ratio regions. On the other hand, the packet error rate and BER performances are lower than compared schemes specially at that regions (Okamoto 2019).

The higher energy efficiency (EF) can be performed by using the MUSA scheme in Device-to-Device (D2D) network communications based on the sphere decoder with SIC receiver. The error probability of device discovery can be reduced by applying MUSA scheme (Hayat 2021).

A new NOMA scheme based on MUSA was proposed by Evren et. al, for mMTC senario and IOT applications. MUSA technique is used to large number of users by using short complex sequences, then the transmitted symbols from all users at the same resource element are spreaded by orthogonal functions with generalized frequncy divison multiplexing waveform to improve system performances in terms of low latency and high user overload with low BER (Evren 2019).

Another method to improve the performance of downlink in 5G systems in terms of SE by using two types of the NOMA techniques. The sum rate in system can be increased in hybrid scheme compared to single scheme of PD NOMA or SCMA at the same symbol rate performance (Sharma 2018).

The MUSA scheme can support high user overload in the uplink transmissions, so it is a promising technology in many applications in 5g and beyond. However, the probability or rate of error increases as UOL increases, which can affect the gains achieved in the system or may not be suitable for some applications, such as those that require high reliability (Yuan 2016).

Allocation powers scheme is needed in PD-NOMA to reduce outage probabilities in downlink, hence better fairness and sum rate performances can be acheived compared to fixed power allocation (Yang 2017). In the same contxt, the maximaization sum rate problem in PD-NOMA downlink system is solved based on the genetic algorithm to find the optimal allocation powers. Thus the proposed scheme outperforms exhaustive and random user pairing algorithms in terms of EF and SE (Alghasmari 2021). To minimize the power consumption in NOMA system, the optimal dynamic user scheduling and power allocation problem was formulated and resolved based on Lyapunov optimization technique (Zhai, 2018). A novel allocation power scheme is proposed to improve EFand fairness at outage probabilities constraints (Cui 2016).

To improve the error propabilty performance in the MUSA uplink, (Ameur *et al.* 2020) suggested finding the optimal allocation of the transmitted power within the constraints of the maximum available power for each device and the total power, taking into account the Succesive Interference cancellation (SIC) decoding threshold related to the error propagation limits. In other words, the PD-NOMA scheme was implemented in the MUSA system because both technologies use the same SIC receiver, where the user overload parameter is 150% and the user locations are fixed in an AWGN channel by the assumption known channel state information. The error propabilty performance of the system compared to an equal transmission power allocation was improved by applying PD-NOMA in the MUSA system and solving the formulated optimization. However, the previous study uses specific complex spreading sequences in the system without evaluating the impact of the cross-correlation between these sequences. In addition, quality of service requirements wasn’t taken into account for each user, i.e. the minimum limits of the desired transmission rates for users.

3. MULTIPLE ACCESS FOR 5G WIRELESS NETWORKS

3.1 Multiple Access Techniques for Current Generations

The first generation is designed to enable and support voice communication for mobile users as the process of delivery takes place between cells (base stations) during voice communication. The first generation uses Frequency Division Multiple Access (FDMA) technology with Frequency Domain Division (FDD) using different international standards such as Nordic Mobile Telephone (NMT) and Advanced Mobile Phone Services (AMPS). Analog Frequency Modulation (FM) and FDD into channels also was relied on a width of 30khz or 10khz by using circuit-switched in a cellular network, which consists of several hexagonal cells, each cell is divided into sectors to increase capacity (Salih 2020). FDMA technologies used in 1G relies on dividing the system's frequency band into several frequency bands separated by guard bands to avoid interference from adjacent bands so that each band is allocated to one user, and remains reserved for the connection duration and it is released when the connection ends to be reused by another user (Goldsmith 2005). This technology suffers from a large waste of bandwidth due to its use of guard bands and thus reduces SE, (Sari 2000).

In the second generation, digital modulation was used to increase the user capacity, as FDMA technology with the dual method of FDD with various international standards such as GSM in, IS_54. G2 supported short messaging services as well as increased capacity and encryption ability to raise security levels compared to the G1. The second-generation initially relied on circuit switching and later moved to networks that were based on packet-switched to increase the capacity of users, so 2.5G (GPRS) and 2.75G (EDGE) generation appeared (Salih 2020). TDMA technology, used in the second generation, allows the transmission to each user on the entire available bandwidth (or narrow bandwidth) for a period, where each frequency channel is divided into time slots as shown in Figure 1.1. Each user is assigned to one or more time quotas through which he can send or receive data, so users are separated in the time domain too. This technology achieves higher SE than FDMA technology and high data transfer rates by allocating several quotas to the same user, in addition to reducing battery consumption by transmitting only within the allocated time quota and silence in the rest of the time quotas. But the difficulty in this technique is in achieving synchronization, and it suffers more from the problems of multiple paths that the signal encounters during its propagation from the transmitter to the receiver, (Goldsmith 2005 and Sari 2000).

The third generation allowed access to the Internet and support data transmission services at higher rates than before, in addition to supporting voice and video services at the same time, through the use of Code Division Multiple Access technology with FDD/TDD with different global standards such as CDM 2000, (UMTS) WCDM. Modulation rank was raised by using 256-QAM modulation instead of 16-QAM modulation, and the power control mechanism was used in 3G networks to reduce interference between users in addition to improving performance in multipath fading channels (Salih, 2020). CDMA technology allows multiple users to share frequency and time resources (shared time and bandwidth), by using special coding based on coding theory, where each user is assigned a code, as shown in Figure 1.1. It consists of a series of binary numbers called a chip. These chips are chosen in a way that achieves the orthogonal property among them to enable the receiver to separate their signals. CDMA technology enables more users to be served within the quota and bandwidth compared to TDMA and FDMA and the possibility of achieving high overload. However, this technology suffers from increased interference between users' signals resulting from the influence of propagation conditions in the channel, which leads to a loss of orthogonality and an increase in the interconnection between the chains, (Goldsmith 2005).

The fourth generation was developed to meet the significant increase in capacity requirements and transmission rates, through the use of OFDMA schems and FDD/TDD with standards such as Long Term Evalution Advanced (LTEA), LTE. This generation allowed greater flexibility in spreading the bandwidth through more options (1.4, 3, 5, 10, 15, and 20Mhz bands), and the transmission time range was reduced to 1ms instead of 2ms in the third generation, which led to a reduction in the delay time latency and improving performance by accelerating the reaction process for changing channel conditions (Salih 2020). OFDMA technology, used in the fourth generation, depends on the orthogonal and hybrid allocation of radio resources in the time and frequency domains as shown in Figure 1.1, where the frequency band is divided into orthogonal subcarriers with narrow bandwidth and very small frequency intervals, which increases the SE and use a flat fade on each sub-frequency channel. OFDMA technology adds a cyclic prefix in a symbol to reduce inter-symbol interference (ISI), thus consuming part of the time resources. However, this technology also suffers from the peak to average power ratio (PAPR) problem in uplink transmissions caused by the nonlinearity of the power amplifiers. To reduce PAPR, single carrier FDMA scheme (SC-FDMA) has been proposed with similar performance to OFDMA but with lower PAPR, where modulated symbols are sent sequentially instead of parallel in OFDMA technology. SC-FDMA technology has been adopted for uplink transmissions in LTE advanced systems, (Goldsmith 2005).

3.2 Fifth Generation Mobile Networks

Previous generations of cellular communication systems supported people's communication with each other and the exchange of a large amount of information among themselves, but with the increasing demand for these systems and the emergence of IoT applications that need to provide large-scale communications for machines and things with or without human intervention such as smart health, smart homes, smart factories, smart manufacturing, smart transportation (Liu 2018) . It was necessary to work on developing a new generation that meets the urgent requirements of these applications by introducing or developing appropriate technologies that can be integrated with wireless communication systems in subsequent generations, so fifth-generation systems must support a data transfer rate with an increase of 10 to 20 times of 4G networks (20Gbps in the downlink and 10Gbps in the uplink), and a connection density of one million connections per square kilometer, in addition to a latency of less than 1ms and mobility of more than 500 km/hour. Therefore, 5G networks need (Akbar 2021):

• Achieving higher capacity and better coverage than achieved in the networks of previous generations, while reducing the complexity and cost of network deployment, especially in high-density networks.

• Possession of a flexible and expandable structure to adapt to the diversity of user and service requirements.
• Achieving flexibility and efficiency by using different spectrum resources including low/high frequency, licensed/unlicensed, pair/unpair, and partition/repartition spectrum.
• Possessing a large capacity to connect devices to deal with the requirements of accessing a large number of IoT devices.
• Improving EE to meet the increasing in data traffic and the diversity of services.
• Reducing the complexity resulting from the use of multiple radio access techniques.
• Achieving smart examples based on knowledge of user behavior and content of services.
• Providing various possible solutions of network security for all types of devices and services in the mobile internet and the IOT.

The International telecommunication union has identified three main expected scenarios of use for 5G cellular systems (Sousa 2018):

1) Enhanced mobile broadband

A high-speed indoor and outdoor communication scenario with uniform quality of service even at cell edges, and includes all applications that require increasingly fast communications such as Virtual Reality, Augmented Reality, and ultra-accurate video communications.

2) Massive machine-type communications (mMTC)

A scenario of connecting a very large number of connected devices with varying QoS requirements to respond to the exponential increase in the density of connected devices. This scenario includes all IoT-related applications such as smart city, smart home, power network monitoring, monitoring applications, and remote control as these services require wide coverage and lower power consumption.

3) Ultra-reliable and low latency communications (URLLC)

A scenario with critical requirements such as latency, response, and packet loss to ensure increased interaction, includes all applications that require high interaction and message delivery assurance such as medical (remote surgery), self-driving, industrial automation, safe transportation applications.

The architecture of the fourth generation system is based on multi-carrier modulation, which is the best choice for channels with large delay dispersion, as it uses orthogonality to achieve the greatest possible efficiency of the used frequency band, but CP-OFDM systems suffer from out of band and CP overhead, which makes them unsuitable as a waveform for some applications. Therefore, improvements to OFDM technology have been made through the use of filtering, windows, and suggesting other waveforms to overcome these challenges, such as Filter Bank Multicarrier Modulation (FBMC). It is similar to the OFDM waveform in terms of dividing the spectrum into orthogonal sub-beams but differs from it by applying a filter to each partial carrier, which leads to greater flexibility in controlling the radiation outside the beam by lowering the side beam level. Thus no need to add a CP or a shielding field, but it suffers from the high complexity of the used filters. Generalized Frequency Division Multiplexing (GFDM) is used in cognitive radio, due to its good sensitizing, spectrum modulation properties, and low PARP compared to OFDM, but with increased receiver complexity. UFMC Universal Filter Multiple Carriers: it uses short-length filters on each sub-beam overcoming the disadvantages of OFDM and FBMC, with higher synchronization requirements, (Vaezi 2018).

The expected scenarios in the fifth generation systems require new advanced technologies to meet their requirements, as the technologies used in previous generations have become unable to achieve the required specifications in some cases, which prompted researchers to develop new technologies that provide new resources and performance to satisfy the requirements and imposed restrictions. Some of these technologies are (Vaezi 2018)

1) Massive multiple input multiple inputcommunications

It depends on the use of a large number of antenna elements used for transmitted or received antenna signals. This technology allows increasing data transfer rates thanks to the spatial modulation Multiplexing and the ability to focus power on a device to optimize the particular link. However, this technology suffers from increased interference between many signals, which can be reduced using the beamforming technique, which directs the beam directly in a specific desired direction using optimal signal processing algorithms. This leads to improved SE.

2) Millimeter Waves Communications

The traditional approved global frequency bands use frequency carriers less than 6GHz, as well as they have reached to inability to meet the rapidly increasing requirements of wireless communication systems, due to complete occupancy of the radio spectrum in this field. Therefore, there is great interest in replacing these fields with Millimeter-wave (mm-wave) frequencies, which allow very wide spectral ranges. Millimeter-wave ranges from 6GHz to 100GHz. It allows to provide wide spectral areas and thus improve the performance of cellular systems, and increase transmission rates. This technology also allows reducing the size of the hardware due to the used small wavelength, but these systems suffer from poor propagation over long distances or across obstacles, which leads to high attenuation, high energy consumption, or a low coverage area. Therefore, this technology is used in small cells, which cover small areas, (Budhiraja 2021).

3) Non-orthogonal multiple access

NOMA schemes are considered as one of the proposed solutions to meet the fifth generation requirements. It can improve SE through users' sharing of radio resources (such as time, frequency, and space resources), in addition to increasing the degree of freedom in the number of non-orthogonal resources. However, these technologies suffer from interference between users' signals due to the absence of orthogonality, which can be reduced by using advanced receivers of high complexity, (Lian 2021).

3.3 Non-Orthogonal Multiple Access Techniques

Theoretically, NOMA differs from orthogonal OMA because of the absence of orthogonality in the management resources method, so any technology that depends on allocating resources to users in a non-orthogonal method is considered a NOMA technology. Some technologies have also been classified under NOMA according to the concept of overloading, which indicates that the number of system users is greater than the number of available system resources, where techniques achieve an overload greater than 100% and are considered as NOMA technologies. However, technologies in which the number of users is less than the number of resources fall under the OMA technologies. For example, when the number of transmitting antennas is greater than the number of users in multiuser communication systems (MU_MIMO), these systems are classified as a NOMA method. CDMA is also considered as NOMA technologies where the number of chips is greater than the number of system users due to overload consideration (Vaezi 2018).

The basic idea of NOMA is using superposition coding for transmitted signals sent in different domains (such as power and symbol). The base station sends a single signal jointly on physical resources in the downlink transmission (DL), which is the superposition of the transmitted signals of the intended users (Bhatia, 2018). Whereas the transmitted signals are accumulated on the same physical resources at the base station in the uplink transmission (UL) to form a single received signal that is handled and the users' signals are separated based on the common design of the transceiver systems. NOMA techniques are classified according to the SC domain into two (Vaezi 2018)

1) Power Domain NOMA schemes

Exploits intensity variation of the received signals caused by the difference in gain of propagation channels between users or even adjust transmission powers to create this variation in case of identical channels. More than one user shares the frequency spectrum allocated for downlink and uplink transmissions, where the base station allocates a portion of the total available power to each user so that the SNIR is different at each user's receiver each user, while the received power levels at the station vary according to each user's channel gain. The successive interference cancellation at the receiver side is used to separate the interfered received signals.The main objective of PD-NOMA is to mitigate the near-distant effect by allocating the far user who has a lower channel gain more power than the near user. It contributes to increasing the SE and achieving a larger capacity compared to orthogonal systems as OMA, but the performance depends on the accuracy of the CSI estimating, which plays a key role in allocating and adjusting the transmission powers to facilitate the work of SIC receiver and reduce the impact of error propagation, (Islam 2017 and Saito 2013).

2) Code Domain NOMAschemes

use different methods at the level of symbols or bits in the transmission side to share the radio-physical resources. Some of these methods spread data on resources using different sparse codebooks in the locations of the non-zero elements, which contain a codeword with a section of its zero elements. Examples of this type are SCMA, PDMA. Another class of CD_NOMA technologies, in which data or modulated symbols are interleaved or scrambled on the resources using scramble chains of different lengths, girding, or recursive patterns such as RSMA, LSSA, IDMA, IGMA. The third group of CD NOMA technologies uses data scattering or modified codes in short or long strings such as GOCA, IDMA, and MUSA, which is the main subject of our research.

The used receiver type varies according to the NOMA technology type used on the transmitting side. Interference cancelation mechanisms are used such as SIC and parallel PIC, or Multi-User Detection (MUD) algorithms such as Minimum Mean Square Error (MMSE), Message passing algorithm, Expectation propagation algorithm and elementary signal estimator , or a combination of both to separate the interfering signals and estimate the transmitted data. For example, a SIC receiver with or without MMSE is used in MUSA and PD-NOMA transmission systems, which can be used in both downlink and uplink (Meng 2018).

Table 3.1 includes some NOMA schemes and the companies working on these schemes, in addition to the level, method of forming signatures in each scheme, type of link that can be used in it, and type of suitable receivers (Dai 2018).

Table 3.1 NOMA schemes (Dai 2018)

NOMA SCHEMES	COMPANY	SIGNATURE	CANDIDATE RECEVIER	DOWNLINK(DL) UNPLINK (UL)
Power domain NOMA	DCM	Power domain superposition	SIC	UL/DL
Sparse code multiple access	Huawei	Symbol level spreading	MPA	UL/DL
Multi-user shared access	ZTE	Symbol level spreading	MMSE-SIC	UL/DL
Pattern division multiple access	CATT	Symbol level spreading	MPA, SIC, SIC-MPA	UL/DL
Low code rate and signature-based shared access	ETRI	Symbol level spreading	MMSE-SIC	UL
Resource spread multiple access	Qualomm	Symbol level scrambling	MMSE-SIC, ESE-PIC	UL
Interleave-grid multiple access	Samsung	Symbol level interleaving	MPA, SIC, SIC-MPA	UL/DL
Interleaver division multiple access	Nokia	Bit-level interleaving	ESE-PIC	UL
non-orthogonal coded multiple access	LGE	Symbol level spreading	MMSE-SIC, ESE-PIC	UL
Non-orthogonal coded access	Nokia	Symbol level spreading	MMSE-SIC, ESE-PIC	UL
Group orthogonal coded access	MTK	Symbol level spreading and scrambling	MMSE-SIC	UL
Low-density spreading-signature vector extension	Fujitsu	Symbol level spreading	MPA, SIC, SIC-MPA	UL/DL
Frequency domain spreading	Intel	Symbol level spreading	MMSE-SIC	UL
Low code rate spreading	Intel	Symbol level spreading	ESE-PIC	UL
Repetition division multiple access	MTK	Symbol level interleaving	MMSE-SIC	UL

4. MULTI USER SHARING ACCESS

NOMA techniques allow many users to share the available resources (frequency, time, code, ...), as it requires that the design of the transmitter and receiver has to be joined and based on the SC principle for the user's signals in the transmitter. In addition to using advanced receivers based on interference cancelation and multi-user detection algorithms. The SE can be improved by using NOMA schemes compared to OMA. It supports a large number of connections by providing new non-orthogonal resources with greater fairness between users, also supporting grant-free transmission systems that reduce latency. These schemes can also be used with OMA schemes and advanced technologies such as massive-MIMO, which leads to achieving greater advantages in the system and meeting the requirements of fifth-generation systems. The PD-NOMA and MUSA schemes are NOMA technologies that improve system throughput, increase the user overload on the same radio resource, and achieve greater flexibility in system resource reuse. Both schemes use the MMSE-SIC receiver to improve decoding performance (Lian 2021).

4.1 MUSA Transmitter

The MUSA scheme can be considered an improvement over CDMA technology, where two schemes depend on multiplexing users' signals in the code domain. MUSA utilizes non-orthogonal complex short spreading sequences to accommodate high UOL in the same radio resources. The complex sequences with short lengths are chosen with good correlation properties (high correlation and low cross-correlation) to enable simple and robust successive interference cancellation at the receiver side and cope with high UOL. MUSA uplink transmissions are suitable for IoT networking applications, where there is a need to reduce the signaling needed to reserve resources and unscheduled at the base station to improve system throughput and reduce latency. MUSA scheme allows a large number of users to send their data on the same radio frequency and time resources without the need for synchronization. The basic idea of the MUSA scheme is shown in Figure 4.1, where each user uses a special spreading sequence then the resulting signals are overlapped at the same resources through the channel. The data for each user can be recovered by applying SIC at the receiver side (Goldsmith 2005).

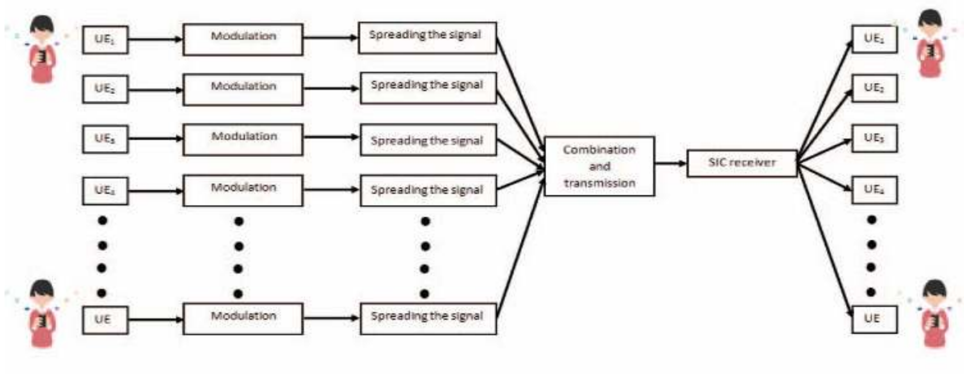

Figure 4.1 Basic principle of MUSA (Eid 2019)

Users share the available radio resources in the MUSA-based communication system, whose number can be arisen by increasing the number of spreading sequences as this number is related to the length of the sequences. The complex elements of spreading sequences have the real and imaginary parts belonging to a set of real numbers such as {-1,1} or {-1,0,1}. The ratio of the number of users to the length of the spreading sequences represents the UOL factor to indicate the number of users who can access the network with a limited number of resources. I.e. the number of users is greater than the number of resource elements available in the system such as time, frequency, etc. UOL factor is given by the following formula (Eid 2019).

$$User\ overloading\ = \frac{Number\ of\ users}{Length\ of\ sequences} \times 100\% \tag{4.1}$$

Equation (4.1) shows that if the length of the sequence is equal to the number of users, then UOL is 100%. On the other hand, if the length of the chain is greater than the number of users, the UOL is less than 100%, so there is no overload on the system. However, if the overload is greater than 100%, the number of users is greater than the number of resources.

The length of complex sequences depends on the number of radio resource elements assigned for each group of users. These sequences are consist of complex numbers from a set of $N_{complex}$ elements, where the real and imaginary parts of each element belong to a real set of N_{real} as shown in figure 4.2. Thus for limited length L we can generate $N_{sequenses}$ complex sequences given as following:

$$N_{sequenses} = \left(N_{complex}\right)^{L} = \left(N_{real}\right)^{2L} \quad (4.2)$$

The base station chooses a set of spreading sequences where its number is equal to the number of users to be served or depending on the desired UOL factor. However, the cross-correlation between these sequences has to be as lower as possible to facilitate the separation of interfering signals at the receiver side.

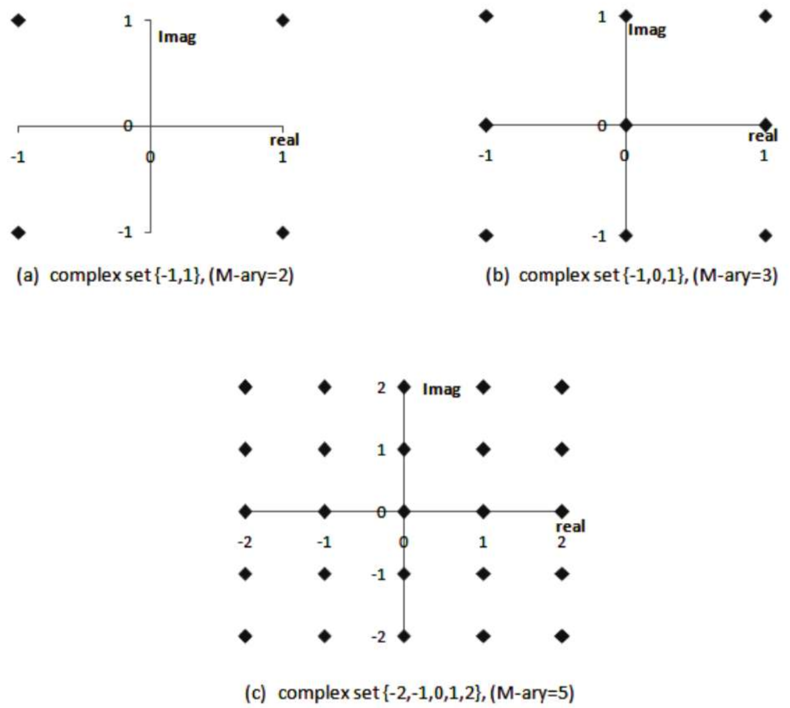

Figure 4.1 Examples for complex elements of the complex spreading sequences (Id 2017)

At the side of each MUSA transmitter, digital modulators are used such as Phase Shift Keying (PSK) or Quadrature Amplitude Modulation (QAM) with a different order, to modify the digital data for each user. The modulated symbols are spread to the specified resource elements by using designed spreading sequences as shown in figure 2.1. In the MUSA downlink, the base station transmits one signal on each resource element, which represents the total sum of users signals components assigned to this resource element and this is called superposition coding. On the other hand, the superposition coding occurs in the MUSA uplink at the base station, where the receiving signal on each component represents the total sum of received components for users' signals. Figure 4.3 shows the superposition coding for six users on four resource elements which means UOL is equal to 300% (Ameur 2021).

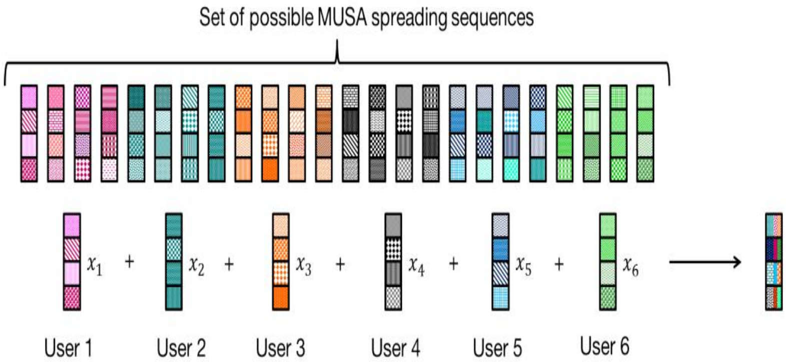

Figure 4.3 The SC for the MUSA system with the UOL = 300%. (Ameur 2021)

MUSA scheme is distinguished by its ability to support high UOL and provide complex sequences as new resources, which in turn increases interference between users and thus low performance. Therefore, advanced receivers are used such as MMSE-SIC due to spreading sequences properties determined premature and well-known at the receiver and transmitter.

4.2 MUSA Receiver

To improve the performance of NOMA systems, the receiver design has to be considered as an essential important factor.The MUSA scheme uses the Successive Interference Cancellation (SIC) technique that employed the difference between desired signal strength and the other signals by reordering users descendingly based on their signal to interference and noise ratios. The basic idea in the SIC receiver is to reconstruct the detected user signal and subtract it from the received signal. The receiver starts to detect the user signal having maximum SINR and considers the other signals as noise as shown in Figure 4.4. Then, the signal will be reconstructed at symbol or codeword level and subtracted from the total received signal to get a new signal without interference resulting from the user's detected signal. This procedure is re-applying on the new signal after rearranging the remaining users in descending order due to the signal to noise ratios until to detect all signals or no signal to be detected. (Meng 2018)

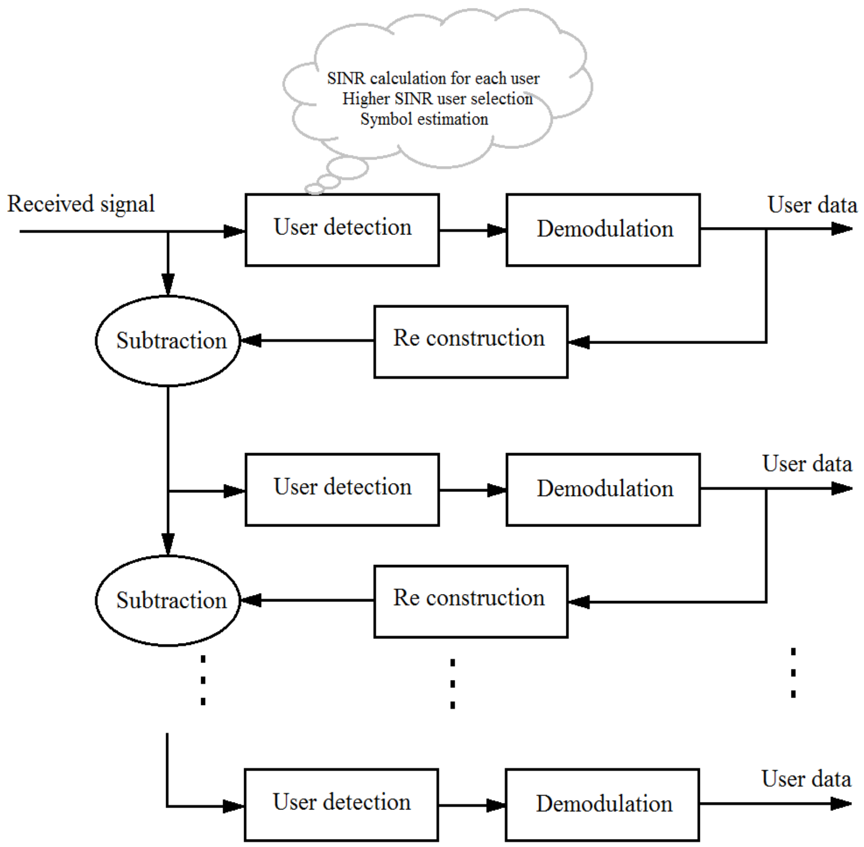

Figure 4.4 SIC receiver structure

The signal can be reconstructed at each stage of interference cancelation by spreading estimated symbols based on the known sequence mapped to each user, but to rebuild signal depending on the estimated codeword achieves the best performance because channel decoding can correct some errors.

Successive interference cancellation receiver requires a detector at each stage to estimate transmitted symbols. MMSE detector is used to achieve the minimum of the mean squared error between the transmitted and estimated symbols to enhance BER performance compared to zero forcing equalizer with SIC, by identifying the weight matrix given in the following formula (Jha 2021).

$$W_{MMSE} = \min_{W} E[\|x - Wy\|^2] \quad (4.3)$$

Where *y,x* represent received signal and transmitted symbols respectively.

MMSE detector is used in linear systems because of its better performance compared with the simple Zero-Forcing (ZF) detector that amplified the noise which leads to low performance (Eid 2019).

SIC receivers suffer from the error propagation problem that results from the wrong detection effect of the previous user signal on the current user signal detection. The error propagation can be reduced by increasing the received power differences of users' signals which can be achieved by large differences between user channels and/or by adjusting the power transmission which in turn increases energy consumption in user devices (Bhatia 2018).

4.3 Power Domain NOMA

NOMA's first appearance was as a proposal from the 3rd generation partnership project (3GPP) to improve downlink in LTEA networks called multiuser superposition transmission (MUST). In the NOMA system, a single signal is received and processed by the receiver's MUD algorithms, unlike other systems such as MIMO that have more than one observation, whether in the downlink or uplink. Multiple users share the resources allocated to the system (frequency, time, code, ...) and the receiver can separate the interfering signals by exploiting the inequality in the received power levels, where the base station allocates more power to the user who has poor CSI in the downlink as shown in figure 4.5a. For the uplink connection shown in figure 4.5b, the poor CSI user transmits with a higher power than the rest of the users to compensate for low gain in the channel to achieve the required quality of service in the uplink (Ali 2016).

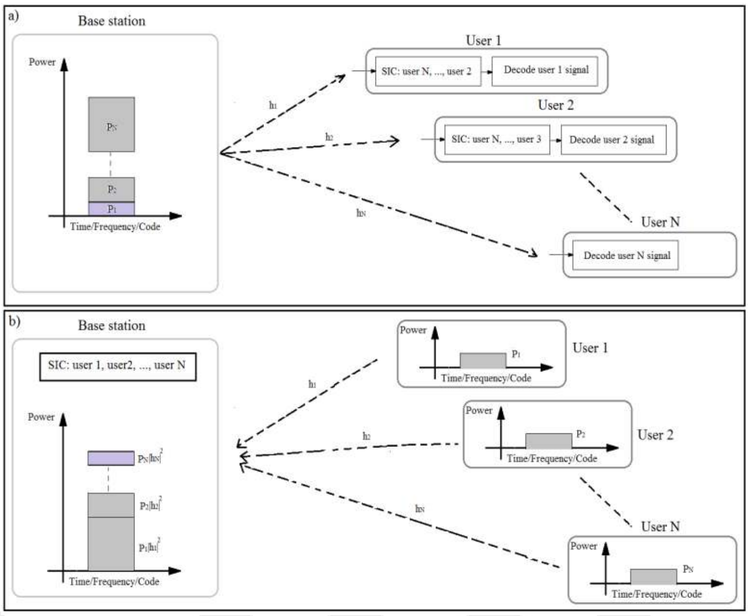

Figure 4.5 a) Downlink PD NOMA b) Uplink PD NOMA

Power domain nonorthogonal multiple access mainly relies on the knowledge of the CSI to determine the appropriate power allocation method to achieve the desired goal as maximizing the sum rate, minimizing outage probability (OP), and maximizing EE (Ali 2016).

The multiuser sharing access scheme allows a large number of users to share the physical resource elements by using nonorthogonal short complex spreading sequences, which are designed with good autocorrelation and low cross-correlation characteristic. MUSA scheme can support higher user load and enable grant free system for mMTC and IoT applications. The main signatures of users in the power domain NOMA are represented by the received power levels at the receiver side. Both NOMA techniques suffer from the high interference between the user's signals compared to OMA systems according to the absence of orthogonality, therefore they need to joint design of transmitter and receiver as we will see in the next chapters.

5. SYSTEM MODEL AND PROPOSED SCHEME

5.1 System Model

Consider a scenario of uplink within a single cell including of a single base station to serve N users sharing L elements of radio resource block (frequency and/or time resources). We assume that the added resources by applying MUSA technology, represented by complex spreading sequences, are allocated in a single unique manner without the collision that occurs when a spreading sequence itself is chosen by more than one user.

The MUSA uplink system consists of a group of transmitters and one receiver as shown in Figure 5.1, where each transmitter modulates the digital data to be transmitted and then spreads it on the available radio resources using short spreading sequences. Practically, the transmitted signals in the uplink are overlapped at the base station receiver, which eliminates the interference between these signals sequentially by SIC technique and estimate the data for each user. But for the designing and performance evaluation, the superposition coding is used to model and simulate this overlap such as shown in Figure 4.1. The resulting signal is passed through a channel which is represented by a model of fading and AWGN, where we assume in this research that the channel parameters are known to the transmitter and receiver. Moreover, we assume that a single antenna is used at the base station receiver and any transmitter.

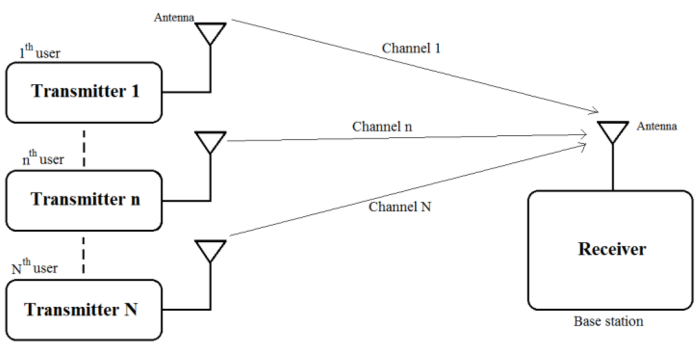

Figure 5.1 System model

The power domain NOMA is applied at each transmitter by adjusting the transmitted power for each user based on the perfect CSI. That allocation powers are utilized at the MMSE_SIC receiver.

5.1.1 Transmitter

Figure 5.2 shows the used transmitter architecture in each device, where each user's binary data sequence is passed to a digital modulator, such as PSK or QAM to convert it into analogue signals represented by a sequence of modulated symbols. Each modulated symbol $x_n$results from modulating a data sequence $d_n$of $(log_2 M) bits$ where M is the order of the used modulation. We consider that the QPSK modulation is used in the system, so the average power of the transmitted symbol can be given as following:

$$E[|x_n|^2] = 1 \tag{5.1}$$

where $n \in \{1, \dots, N\}$, is the number of users, and $x_n$is the modulated symbol transmitted by the n^{th}user.

Each modulated symbol $x_n$is spread on a resource block of L elements using a complex spreading sequence of L complex elements, which are selected from the set of sequences already designed in the base station to control resource management in the system, and allocated each user a unique sequence. Let us suppose that the set of complex spreading sequences is defined by the matrix S = $[s_1, \dots, s_n, \dots, s_N]$with dimensions $(L \times N)$ and that the sequence $\boldsymbol{s}_n$, represented by the n^{th}column of **S** matrix, is allocated to the n^{th}user. So the signal vector $\boldsymbol{y}_n$ generated by applying MUSA scheme in the n^{th}user's transmitter can be written as following:

$$y_n = x_n s_n, \;\; n \in \{1, \dots, N\} \tag{5.2}$$

where x_n is the modulated symbol transmitted by the n^{th} user, $s_n = [s_n(1), \dots, s_n(l), \dots, s_n(L)]^T$ the spreading sequence assigned to the n^{th}user, and $y_n =$

$[y_n(1), \ldots, y_n(l), \ldots, y_n(L)]^T$, where $y_n(l) = x_n s_n(l)$ is the transmitted signal of the n^{th}user on the l^{th} resource element and $l \in \{1, \ldots, L\}$.

In order to implement the PD NOMA scheme, each user transmits its signals with a transmitted power p_n, which is allocated by the base station depending on the propagation channel conditions of each user. The transmitted power p_n does not exceed the maximum power in each device, which we assume is equal for all users $(p_n \leq p_{max}, \forall n)$. The transmitted signal $t_n(l)$ for n^{th}user on the l^{th} resource element can be written in the following form:

$$t_n(l) = \sqrt{p_n} y_n(l) = \sqrt{p_n} x_n s_n(l), \quad n \in \{1, \ldots, N\} \tag{5.3}$$

So the transmitted signal vector from the n^{th}user on the resource block is:

$$t_n = \sqrt{p_n} y_n, \quad n \in \{1, \ldots, N\} \tag{5.4}$$

where $p_n$is the transmitted power allocated to the n^{th}user, $\boldsymbol{y}_n$is the output signal vector resulting from the MUSA implementation at the n^{th} transmitter given in (5.2) and $t_n = [t_n(1), \ldots, t_n(l), \ldots, t_n(L)]^T$ where $t_n(l)$ is given by (5.3).

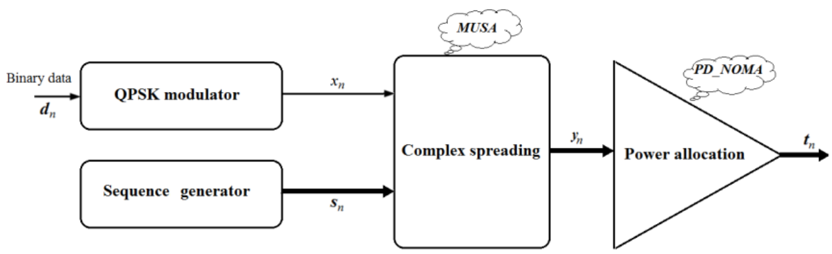

Figure 5.2 Block diagram of one transmitter

The transmitted signals shown in (5.4) for each user is propagated through a fading channel modeled by complex vector $h_n = [h_n(1), \ldots, h_n(l), \ldots, h_n(L)]^T$,whose elements are the channel gain on each l^{th} resource element. Each transmitted signal $t_n(l)$ from user n is multiplied by the corresponding channel complex gain $h_n(l)$ on the resource element l. All generated and transmitted signals are combined on the same resource element and AWGN samples added. Thus, the received signal $r(l)$ on the l^{th} resource element will be as following:

$$r(l) = \sum_{n=1}^{N} h_n(l) t_n(l) + u(l), \;\; l = 1, \dots, L \tag{5.5}$$

where $h_n(l)$is the n^{th} users's channel gain on the l^{th} resource element, $t_n(l)$is the n^{th} users's transmitted signal on the l^{th} resource element given in (5.3) and $\boldsymbol{u}(l)$ is AWGN vector samples u**,** where u~CN$(0, \sigma^2 I_L)$. Using (5.3) into (5.5) and supposing that the user's transmitted symbols vector is $x = [x_1, \dots, x_n, \dots, x_N]^T$, the relation (5.5) becomes as following:

$$r(l) = a_l x + u(l), \;\; l = 1, \dots, L \tag{5.6}$$

where $a_l = [a_l(1), \dots, a(n), \dots, a_l(N)]$ is a row consisting of N elemesnts and each element is given as following:

$$a_l(n) = \sqrt{p_n} s_n(l) h_n(l), \;\; l = 1, \dots, L \; and \; n = 1, \dots, N \tag{5.7}$$

where $h_n(l)$ is the n^{th} users's channel gain on the l^{th} resource element, p_n is the transmitted power allocated to the n^{th}user, and $s_n(l)$ is the l^{th} complex element number of the spreading sequence $\boldsymbol{s}_n$ assigned to the n^{th}user.

Thus, the received signal vector r, over all the resource block can be written as following:

$$r = Ax + u \tag{5.8}$$

where $r = [r(1), \dots, r(l), \dots, r(L)]^T$, $r(l)$ given in (5.6), $x = [x_1, \dots, x_n, \dots, x_N]^T$ is the user's transmitted symbols vector, u is the AWGN vector where u~CN$(0, \sigma^2 I_L)$, and A is a matrix with dimensions $(L \times N)$ whose elements $a_l(n)$are given by the relation (5.7).

5.1.2 Receiver

The MUSA receiver uses a SIC algorithm with the MMSE linear detector in each SIC stage for multiuser detection. The same technology is used in the PD-NOMA receiver, where the remaining users in each SIC stage are arranged in descending order according to the correspond SINRs. The MMSE_Ordered-SIC (MMSE_OSIC) receiver is used to separate the interfering signals and estimate the transmitted user data for the received signal model given in (5.8). The structure of the MMSE_OSIC receiver is shown in Figure 4.4, which starts operating from the received signal $\boldsymbol{r}$, according to the following steps:

1) User detection

In this stage, the users are arranged and the modulated transmitted symbols are estimated based on the MMSE linear detector, where the weight matrix $W_{MMSE}$is initially calculated according to the relation (4.3) as follows:

$$W_{MMSE} = (A^H A + \sigma^2 I_N)^{-1} A^H \quad (5.9)$$

where A is a matrix with dimensions (L×N)whose elements al (n) are given in (5.7), A^H is the complex conjugate of the transposon matrix A, and I_N is a neutral matrix with dimensions (N×N). The weight matrix computed with (5.9) is used to calculate the SINRs for all users as following: (Goldsmith 2005)

$$\gamma_n = \frac{|w_{n,MMSE} A_n|^2}{\sum_{m \neq n} |w_{n,MMSE} A_m|^2 + \sigma^2 \|w_{n,MMSE}\|^2} \quad (5.10)$$

where γ_n is the signal to interference and noise ratio for the n^{th} user, A_n is the n^{th}column of matrix A, A_m is the m^{th}column of matrix A, $w_{n,MMSE}$ is the n^{th}row of matrix W_{MMSE} given in (5.9), $n \in \{1, \ldots, N\}$ and $m \in \{1, \ldots, M\}$where $n \neq m$.

After obtaining the all SINRs, the users are arranged in descending order and the receiver chooses the first user, i.e. the highest SINR, to estimate its transmitted symbol. Assuming that k^{th} user is the highest SINR, the estimated transmitted symbol $\hat{x}_k$ for k^{th} user can be estimated as following:

$$\hat{x}_k = w_{k,MMSE}r \tag{5.11}$$

where $k \in \{1, \dots, N\}$, $w_{k,MMSE}$ is the k^{th} row of the W_{MMSE} matrix given in (5.9), and $\boldsymbol{r}$ is the received signal vector given in (5.8).

2) Demodulation

The QPSK demodulator is applied to the estimated symbol $\hat{x}_k$ resulting from (5.11) to get the estimated binary data $\hat{d}_k$ which is used to reconstruct the signal of k^{th} user. It is possible to use the estimated symbol $\hat{x}_k$ shown in (5.11) directly without the need of demodulation, but this may cause additional errors in the system due to the error propagatin in the next stages. We call $\tilde{x}_k$ as the modulated symbol signal resulting from the modulation of the estimated binary data $\hat{d}_k$ corresponding to the k^{th} user.

3) Reconstruction

The estimated binary data $\hat{d}_k$ is modulated using the QPSK modulator and the resulting modulated symbol is spread with the complex sequence assigned to the k^{th} user. The reconstructed signal $\hat{t}_k$ for k^{th} user at this stage is given by the following formula:

$$\hat{t}_k = \tilde{x}_k s_k \tag{5.12}$$

where $\tilde{x}_k$ is the estimated modulated symbol resulting from step B by modulating the estimated binary data $\hat{d}_k$, and s_k is the complex spread sequence allocated to the k^{th} user.

4) Subtraction

At this step, the interference, resulting from k^{th} user signal, is eliminated from the total received signal vector $\boldsymbol{r}$ as following:

$$\hat{r} = r - \hat{t}_k \tag{5.13}$$

where $\hat{r}$ is the received signal including the remaining signals after removing the k^{th} user signal from the received signal r given in (5.8), and $\hat{t}_k$ is the estimated k^{th} user signal which is reconstructed in the receiver by the formula (5.12).

Steps A through D represent the first SIC stage in which a user's data is estimated and decoded, then the interference resulting from that user's signal is removed to obtain a new received signal vector $\hat{r}$ with the same dimensions of vector $\boldsymbol{r}$ as shown in (5.13). The new received signal vector $\hat{r}$ can be re-represented in a form similar to the model of the received signal vector r shown in (5.8) as following:

$$\hat{r} = \hat{A}\hat{x} + \hat{u} \tag{5.14}$$

where $\hat{A}$ is a matrix with dimensions $(L \times (N-1))$that results by removing the k^{th} column from the matrix A with dimensions $(L \times N)$and its elements $a_l(n)$ given in (5.7), $\hat{\boldsymbol{x}}$ is a column of length $(N-1)$ represents the remaining users' modulated symbols resulting from vector x by removing the k^{th} element in it, and $\hat{u}$ is AWGN vector where $\hat{u}$~CN$(0, \sigma^2 I_L)$.

In the next SIC stage, steps A through D are applied to the new received signal $\hat{r}$ shown in (5.14) to estimate and decode another user's data and eliminate its interference from to the new received signal $\hat{\boldsymbol{r}}$. Thus, this procedure is repeated until all users' data are estimated or there is no signal to be processed.

5.2 Problem Formulation

The performance of the modeled system in the previous paragraph depends mainly on the signal to interference and noise ratio. If this ratio increases, the BER for each user decreases and the rate for each user increases. This is because of that the error probability for each user can be approximated by the following formula: (Shengli 2003)

$$BER_n \approx \frac{1}{5} e^{-\gamma_n/2} \tag{5.15}$$

Where γ_n is the signal to interference and noise ratio for the n^{th} user given by (5.10) Also, $n \in \{1, \dots, N\}$. Depending on (5.15), the average error probability is as follows:

$$BER \approx \frac{1}{5N} \sum_{n=1}^{N} BER_n \tag{5.16}$$

Where BER_n is error probability for the n^{th} user given by (5.15), and N is the number of users. On the other hand, the rate for each user is given (estimated in (b/s/Hz)) with the following formula:

$$R_n = log_2(1 + \gamma_n) \tag{5.17}$$

Where γ_n is the signal to interference and noise ratio for the n^{th} user given by (5.10) thus the average rate and sum rate are given, respectively, as follows?

$$R_{ave} = \frac{1}{N} \sum_{n=1}^{N} R_n \tag{5.18}$$

$$R_{sum} = \sum_{n=1}^{N} R_n \tag{5.19}$$

Where R_n is the rate for the n^{th} user given by (5.17).

The values of the signal to interference and noise ratio γ_n shown in (5.10) are related to the following parameters: Noise power σ^2, user channel gain coefficients $h_n = [h_n(1), \dots, h_n(l), \dots, h_n(L)]^T$, auto-correlation and cross-correlation characteristics for the matrix of complex spreading sequences $\mathrm{S} = [s_1, \dots, s_n, \dots, s_N]$, and the transmitted allocated powers to users represented by the array $P = [p_1, \dots, \mathrm{p}_n, \dots, \mathrm{p}_N]$.

Depending on the assumption that the perfect CSI and that the noise power is known, so it is possible to raise the values of the signal to interference and noise ratio by designing complex spreading sequences and allocating powers in an suboptimal manner, which contributes to improve the required performance standards such as transmission rates and error probability. The process of designing spreading sequences starts from choosing a set of real numbers to form a complex elements set from which a large number of complex spreading sequences $N_{sequenses}$ can be designed as shown in (4.2). Therefore, choosing a complex spreading sequences matrix with optimal auto- correlation and cross-correlation characteristics, requires a highly complex search procedure because the number of possible options to form that matrix with N columns is: $C_N^{N_{sequenses}} = \frac{N_{sequenses}!}{N!\,(N_{sequenses}-N)!}$. For example, assuming that the set shown in Figure (4.2a) where $N_{real} = 2$ and $N_{complex} = 4$, and the number of users is $N = 6$ and the length of the sequences $L = 4$, so the number of sequences that can be formed is $N_{sequenses} = 256$. Thus the number of possible options for the matrix **S** is $C_N^{N_{sequenses}} \sim 10^{11}$. This example shows the ineffectiveness of this method for designing complex spreading sequences in the real time because it would increase latency and power consumption to process those large number of options.

Based on the foregoing, in this thesis we will assume that the selection of complex spreading sequences matrix is already and randomly done, and interest will be to allocate these sequences and transmission power according to the CSI. The main goal is to increasing the minimum signal to interference and noise ratio to achieve a suboptimal fairness among users in terms of transmission rate and error probability within the required minimum rate and the available maximum power constraints for each user. In other words, the problem (P1) can be formulated to find the best arrangement of the columns of the matrix S and the values of the transmitted powers as follows:

(P1) Objective: $\underset{\boldsymbol{P},\boldsymbol{S}}{max} \underset{n\in\{1,\dots,N\}}{min} \{\gamma_n\}$ (5.20)

$$\text{subjet to:} \begin{cases} 0 \leq p_n \leq p_{max}, \ \forall n \\ R_n \geq R_{min}, \\ \left|max\,\{R_n\}_{n=1}^{\boldsymbol{N}} - min\,\{R_n\}_{n=1}^{\boldsymbol{N}}\right| \leq \varepsilon, \\ n \in \{1, \dots, N\} \end{cases}$$

Where γ_n is the signal to interference and noise ratio for the n^{th} user given by (5.10). for each $n \in \{1, \dots, N\}$, R_n is the transmission rate for the n^{th} user given by (5.17), R_{min} is the required minimum transmission rate for each users where we assume that the QoS requirements for all users are equal in terms of transmission rate, p_{max} is the available maximum power in devices, ε is the maximum variance margin between transmission rates (to be determined later), $P = [p_1, \dots, p_n, \dots, p_N]$ are the transmitted powers of users, and $\boldsymbol{S}$ is the complex spreading sequences matrix. It should be noted here that the columns of the matrix produced by solving the problem (P1) are the same as the columns of the previously designed matrix, but with an order that may differ from them.

The problem (P1) is feasible if the maximum power p_{max} is sufficient to satisfy the required minimum transmission rate R_{min} constraint. At least, the maximum power p_{max}must be greater than the maximum power, which achieves the required rate R_{min} considering the cross-correlation between the sequences is zero, i.e.:

$$p_{max} > \max\left\{p_i \middle| log_2\left(1 + \frac{p_i\left|\boldsymbol{h}_{\mathrm{i}}{}^{\mathrm{H}}\,\boldsymbol{s}_i\right|^2}{\sigma^2}\right) = R_{min}, n \in \{1, \dots, N\}\right\} \quad (5.21)$$

Where R_{min} the required minimum is rate for all users, and p_{max} is the available maximum power in devices. In this project, we will choose the values of the maximum power p_{max} based on the OMA benchmark to satisfy the condition (5.21).

The formulated problem is not linear and non-convex constraints and it is difficult to solve so we will work to find an approximate solution separately for sequences matrix order and transmission powers by using iterative algorithms.

5.3 Sequences Allocation Algorithm

In this stage, we assume that the allocated power for each user is equal to the available maximum power ($p_n = p_{max}, \ \forall n,$), in addition to the perfect CSI and the initial complex spreading sequences matrix. So the target will be to assign each user with a unique sequence to achieve the objective in (5.20) by computing the signal to interference and noise ratios for all possible permutations, then selecting the optimal allocation at which the achievable minimum rate is maximum. This procedure can be implementation by applying SIC receiver shown in figure 4.4 with remove the demodulation, re-construction and symbol estimation blocks. But the number of all possible permutations is related to the number of users$N$, and it increases as N increases, where the number of all possible permutations is equal to $N!$. This means a partial application of $N!$ times for the SIC receiver, including calculating the signal to interference and noise ratios, which leads to a high complexity especially with the increase in the number of users, for example, for $N = 6$ =>$N! = 720$, and for $N = 8$ =>$N! = 40320$.

Therefore, we propose the iterative Algorithm2 shown in Table 5.2, which is limited to the maximum number of iterations t_1 to reduce the complexity. Because Algorithm2 need to calculate the signal to interference and noise ratios more than one, we propose the Algorithm1 shown in Table 5.1 which is a function gives the order of users according to the detection process succession and determines the signal to interference and noise ratios for a specific allocation of spreading sequences by using (5.9) and (5.10) and modeling the receiver residual signal (5.14) at each SIC stage.

Table 5.1 Algorithm1 to calculate the SINRs and find detection order

Input: Spreading sequences matrix S, Allocated powers $\sqrt{\mathbf{P}}$**,** Channel coefficients matrix $\boldsymbol{h} = [\boldsymbol{h}_1, \dots, \boldsymbol{h}_n, \dots, \boldsymbol{h}_N]$ **,** Number of user N, Noise power σ^2, Length of sequences L.
Output: SINR array for all users $\boldsymbol{\gamma}$, Detection order array $\boldsymbol{K}$.
Steps: 1. Compute elements of matrix $\boldsymbol{A}$ using Eq. (5.7). 2. **for** $n = 1$ **to** $n = N$ **reapeat** 3. Calculate weight matrix $\boldsymbol{W}_{MMSE}$ using Eq. (5.9). 4. Calculate SINR (γ_n) for $(N - (n - 1))$ users using Eq. (5.10). 5. Find the maximum SINR (γ_k) and k the number of correspond user. 6. Insert γ_k into the output array $\boldsymbol{\gamma}$**.** 6. Insert k into the output array $\boldsymbol{K}$**.** 6. Remove the k^{th}column from matrix $\boldsymbol{A}$**.** 9. **end for**

Initially, the signal to interference and noise ratios are calculated using Algorithm1 shown in Table 5.1, where the first user is allocated to the first spreading sequence represented by the first column of the original matrix S**,** while the second column sequence is allocated to the second user and so on until the last column is allocated to the N^{th} user. The user-detection order, resulting from the application of Algorithm1, is also used to form the next spreading sequences matrix in a different order from the original matrix S, where the first user in the next stage is allocated to the spreading sequence that was allocated to the first detected user in the current stage, and the spreading sequence of the second detected user in the current stage is allocated to the second user in the next stage, and so on. That is, the positions of the columns of the original matrix are shifted depending on the detection order. The minimum signal to interference and noise ratio in the current stage are compared with the minimum SINR in the next stage. Then the best sequences allocation is selected according to the maximum minimum signal to interference and noise ratio between the current and next stage. Thus, the procedure is repeated until the number of repetitions becomes larger than the maximum number of iterations t_1.

Table 5.2 Algorithm2 to find the near optimal sequences allocation

Input: Spreading sequences matrix **S**, Allocated powers $\sqrt{\mathbf{P}}$**,** Channel coefficients matrix $\boldsymbol{h} = [\boldsymbol{h}_1, \dots, \boldsymbol{h}_n, \dots, \boldsymbol{h}_N]$ **,** Number of user N, Noise power σ^2, Length of sequences L, Maximum number of iterations t_1.
Output: Near optimal sequences matrix $\boldsymbol{S}_{opt}$.
Steps: 1. Compute $\gamma_n^{(0)}$for each user and find detection order $\boldsymbol{k}^{(0)}$ by aplying Algorithm1. 2. $\boldsymbol{S}_{opt} \leftarrow \boldsymbol{S}$. 3. $\gamma_{min}^{(0)} \leftarrow \min_{n\in\{1,..,N\}}\left\{\gamma_n^{(0)}\right\}$. 4. Reorder the columns of matrix according to $\boldsymbol{k}^{(0)}$. $\boldsymbol{S}^{(0)} \leftarrow \boldsymbol{S}(:, \boldsymbol{k}^{(0)})$ 5. **for** $t = 1$ **to** $t = t_1$ **Reapeat** 6. Compute $\gamma_n^{(1)}$for each user and find detection order $\boldsymbol{k}^{(1)}$ by aplying Algorithm1 for new sequences matrix $\boldsymbol{S}^{(0)}$. 7. $\gamma_{min}^{(1)} \leftarrow \min_{n\in\{1,..,N\}}\left\{\gamma_n^{(1)}\right\}$. 8. **if** $\gamma_{min}^{(1)} > \gamma_{min}^{(0)}$ **Then** $\boldsymbol{S}_{opt} \leftarrow \boldsymbol{S}^{(0)}$. $\gamma_{min}^{(0)} \leftarrow \gamma_{min}^{(1)}$. **End if.** 9. $\boldsymbol{S}^{(0)} \leftarrow \boldsymbol{S}(:, \boldsymbol{k}^{(1)})$. 10. **end for**

The performance of Algorithm2 in terms of improving the minimum signal to interference and noise ratios is related to the number of iterations t_1 and the user channel gains. It is possible that the near optimal solution resulting from this algorithm is the same as the original random allocation represented in the original complex spreading sequences matrix S.

5.4 Power Allocation Algorithm

The proposed algorithm in this stage aims to find the near optimal transmission powers that achieve the objective of the problem (P1) at the complex spreading sequence matrix resulting from the application of Algorithm2 or any specific matrix. That is, the problem (P1) can be reformulated as follows:

(P2) Objective: $$\max_{\boldsymbol{P}} \min_{n\in\{1,\dots,N\}} \{\gamma_n\} \tag{5.22}$$

$$subjet\ to: \begin{cases} 0 \le p_n \le p_{max}, \ \forall n \\ R_n \ge R_{min}, \\ \left|max\,\{R_n\}_{n=1}^{N} - min\,\{R_n\}_{n=1}^{N}\right| \le \varepsilon, \\ n \in \{1,\dots,N\} \end{cases}$$

Where γ_n is the signal to interference and noise ratio for the n^{th} user given by (5.10). for each $n \in \{1, \dots, N\}$, R_n is the transmission rate for the n^{th} user given by (5.17), R_{min} is the required minimum transmission rate for each users where we assume that the QoS requirements for all users are equal in terms of transmission rate, p_{max} is the available maximum power in devices, ε is the maximum variance margin between transmission rates (to be determined later), and $P = [p_1, \dots, p_n, \dots, p_N]$ are the transmitted powers of users.

Reducing the signal to interference and noise ratio γ_n corresponding to each user is achieved by decreasing the power of the transmitted signal p_n, which in turn leads to an increase in the corresponding signal to interference and noise ratios for users detected in the next SIC deletion stages (users with the lowest signal to interference and noise ratio in the current user detection stage). Because the problem (P2) is still non-convex and non-linear and it is difficult to find a closed solution, we will work on designing an iterative algorithm based on the maximum values of transmission powers $p_n = p_{max}, \ \forall n \in \{1, \dots, N\}$, where the corresponding signal to interference and noise ratio are initially calculated for these powers using the Algorithm1 shown in Table 5.1, then from which the transmission rates for all users will be calculated. Suppose user $j \in \{1, \dots, N\}$ has the lowest signal to interference and noise ratio, i.e. the lowest transmission rate. Therefore, the powers allocated to the rest of the users must be reduced so that the transmission rates are equal to the average rates for all users, i.e. it must be:

$$R_m(\acute{P}) = \frac{1}{N}\sum_{n=1}^{N} R_n(P)\,,\ \ m \neq j \tag{5.23}$$

where $P = [p_1, \dots, p_n, \dots, p_N]$ is the transmitted allocated powers to users at the current iteration, $\acute{P} = [\acute{p}_1, \dots, \acute{p}_{j-1}, p_j, \acute{p}_{j+1}, \dots, \acute{p}_N]$ is the transmitted allocated powers to users at the next iteration, $R_n(P)$ is the transmission rate for the n^{th} user given in (5.17) at the values of the powers P, $R_m(\acute{P})$ is the transmission rate for the m^{th} user given in (5.17) at the values of the powers $\acute{P}$ where $j \neq m \in \{1, \dots, N\}$ and $j \in \{1, \dots, N\}$ is the user number with the minimum signal to interference and noise ratio (as well as the minimum rate) and is calculated as follows:

$$j = \left\{ i \,|\, \gamma_i(P) = \min_{n \in \{1,\dots,N\}} \{\gamma_n(P)\}, i \in \{1, \dots, N\} \right\} \tag{5.24}$$

Where $\gamma_n(P)$ and $\gamma_i(P)$ are the signal to interference and noise ratios for the $n^{th}$and i^{th}users, respectively, and given by (5.10) at the values of the current iteration powers$P = [p_1, \dots, p_n, \dots, p_N]$. It is noted that at current iteration, the power allocated to the j^{th}user is not changed because the goal is to increase the signal to interference and noise ratio for this user, therefore its power should not be reduced. Starting from (5.23) and using (5.17), we have:

$$R_m(\acute{P}) - \frac{1}{N}\sum_{n=1}^{N} R_n(P) = log_2\left(1 + \gamma_m(\acute{P})\right) - \frac{1}{N}\sum_{n=1}^{N} log_2(1 + \gamma_n(P)) = log_2\left(1 + \gamma_m(\acute{\boldsymbol{P}})\right) - log_2\left(\prod_{n=1}^{N}(1 + \gamma_n(\boldsymbol{P}))\right)^{1/N} = 0 \tag{5.25}$$

So, the signal to interference and noise ratio $\gamma_m(\acute{P})$ for the m^{th} user at the values of the powers $\acute{P}$, can be rewritten as following:

$$\gamma_m(\acute{P}) = \left(\prod_{n=1}^{N}(1 + \gamma_n(P))\right)^{1/N} - 1,\ \ m \neq j \tag{5.26}$$

Where $\gamma_n(P)$ is the signal to interference and noise ratio for the n^{th} user given in (5.10) at the values of the powers P, and $j \in \{1, \dots, N\}$ is the user number with the minimum signal to interference and noise ratio at current iteration ginen in (5.24). Because of the difficulty of solving the set of nonlinear equations shown in (5.25) for $j \neq m \in \{1, \dots, N\}$ we assume the following approximations:

$$\gamma_m(\acute{P}) = \acute{p}_m \beta_m(\acute{P}) \ , \ \ m \neq j,$$

$$\gamma_m(P) = p_m \beta_m(P) \, , \ \ m \neq j,$$

$$\beta_m(\acute{P}) \approx \beta_m(P) \, , \ \ m \neq j,$$

Where p_m and $\acute{p}_m$ are the powers allocated to user $m \in \{1, \dots, N\}$ in the current itration and the next iteration, respectively. The approximation imposed in (5.26) results from neglecting the effect of the power allocated to the user m on the denominator of (5.10) compared to its effect on the numerator.

$$\frac{\gamma_m(\acute{P})}{\gamma_m(P)} \approx \frac{\acute{p}_m}{p_m} \ , \ \ m \neq j \qquad (5.27)$$

Substituting (5.27) into (5.25), we find the approximate values of the allocated powers to the next iteration $\acute{P}$, as follows:

$$\acute{p}_m = \begin{cases} \left(\left(\prod_{n=1}^{N} \left(1 + \gamma_n(P) \right) \right)^{1/N} - 1 \right) / p_m, & m \neq j \\ p_m, & m = j \end{cases}, \qquad (5.28)$$

where p_m and $\acute{p}_m$ are the powers allocated to user $m \in \{1, \dots, N\}$ in the current itration and the next iteration, respectively, is the signal to interference and noise ratio for the n^{th} user given in Equation (5.10) at the values of the powers P, and $j \in \{1, \dots, N\}$ is the user number with the minimum signal to interference and noise ratio at current iteration given in Equation (5.24). Depending on the foregoing, the iterative Algorithm3 presented in Table 5.3 is proposed with a maximum number of iterations t_2 to find the near optimal powers allocation for the problem (P2).

Table 5.3 Algorithm3 to find the near optimal powers allocation

Input: Spreading sequences matrix **S**, Length of sequences L, Noise power σ^2,
Channel coefficients matrix $\boldsymbol{h} = [\boldsymbol{h}_1, \dots, \boldsymbol{h}_n, \dots, \boldsymbol{h}_N]$, ε from Eq. (5.34)
Number of user N, Maximum power $\sqrt{P_{max}}$ from Eq. (5.32),
Maximum number of iterations t_2, The required minimum rate R_{min}.

Output: Near optimal power allocation $\sqrt{\boldsymbol{P}_{opt}}$.

Steps:

1. Set any power in $\sqrt{\boldsymbol{P}} = [\sqrt{p_1}, \dots, \sqrt{p_n}, \dots, \sqrt{p_N}]$ to maximum.
   $\sqrt{p_n} \leftarrow \sqrt{P_{max}}$ for any $n \in \{1, \dots, N\}$.
2. $\sqrt{\boldsymbol{P}_{opt}} \leftarrow \sqrt{\boldsymbol{P}}$
3. $t \leftarrow 0$
4. **while** $t \leq t_2$ **reapeat**
5. $t \leftarrow t + 1$
6. Compute $\gamma_n^{(0)}$ for each user by aplying Algorithm1.
7. Calculate $R_n^{(0)}$ for each user using Eq. (5.17) at $\gamma_n^{(0)}$.
8. Find j using Eq. (5.24) at $\gamma_n^{(0)}$.
9. Calculate $\sqrt{\acute{\boldsymbol{P}}} = [\sqrt{\acute{p}_1}, \dots, \sqrt{\acute{p}_{j-1}}, \sqrt{p_j}, \sqrt{\acute{p}_{j+1}}, \dots, \sqrt{\acute{p}_N}]$ using Eq. (5.28) at $\gamma_n^{(0)}$.
10. **if** $\sqrt{\acute{p}_n} > \sqrt{P_{max}}$ **Then**
    $\sqrt{\acute{p}_n} \leftarrow \sqrt{P_{max}}$.
11. **end if**
12. $\sqrt{\boldsymbol{P}_{opt}} \leftarrow \sqrt{\acute{\boldsymbol{P}}}$
13. Calculate $\varepsilon_0 = |max\{R_n^{(0)}\} - min\{R_n^{(0)}\}|$.
13. **if** $\varepsilon_0 \leq \varepsilon$ **Then** stop.
14. **else** continue
15. **end if**
16. **end while**

The values of the powers $\acute{P}$ required to the next iteration are calculated using (5.28) based on the values of the powers P allocated in the current iteration. Resulting power values from (5.28) are verified that they do not exceed the value of the maximum power (P_{max}), and then the algorithm shown in Table 5.1 is used to calculate the signal to interference and noise ratios and rates corresponding to the calculated powers $\acute{P}$ in order to check the constraint (5.22a) in the problem (P2). The allocated power values for the next iteration are recalculated according to power values $\acute{P}$ (array P is replaced by array $\acute{P}$ which will recalculated again). The algorithm will stop in case of exceeding iteration number t_2 or achieving the constraint 5.22c in the problem (P2).

5.5 OMA Benchmark Scheme

The OMA scheme is used as a reference to evaluate the performance of the proposed system and to determine ε value in the constraint (5.20c) in the problem (P1), in addition to determining the value of the maximum power P_{max}. Assuming that the physical resources are divided equally among the users in the OMA scheme, the portion $\alpha_n = 1/N$ is allocated to each user such that $\sum_{n=1}^{N} \alpha_n = 1$ and $0 < \alpha_n \leq 1$. Thus the signal-to-noise ratio SNR_n for the user n can be written as:

$$SNR_n = \frac{p_n^{OMA}|h_n^{OMA}|^2}{\alpha_n \sigma^2} \quad ,n \in \{1, \dots, N\} \tag{5.29}$$

Where N is the number of users, p_n^{OMA} is the transmitted power from the n^{th} user in OMA scheme, $|h_n^{OMA}|^2$ is the n^{th} users's channel gain in OMA scheme, $\alpha_n = 1/N$ is the allocated part of physical resources for the n^{th} user in OMA scheme , and σ^2 is the noise power.

Thus, the user's transmission rate R_n^{OMA} for the user n, is calculated in the OMA scheme as follows:

$$R_n^{OMA} = \alpha_n log2(1 + SNR_n) \quad ,n \in \{1, \dots, N\} \tag{5.30}$$

Where SNR_n is the signal-to-noise ratio for the the n^{th} user shown in (5.29), and $\alpha_n = 1/N$. The required minimum power for all OMA users is calculated so that the transmission rate R_n^{OMA} for each user is equal to the minimum required transmission rate R_{min} based on (5.29) and (5.30) . Thus required minimum power $p_{n,min}^{OMA}$ can be written as follows:

$$p_{n,min}^{OMA} = \{p_n^{OMA} |\, R_{min} = R_n^{OMA}\} = \left(2^{R_{min}/\alpha_n} - 1\right) \frac{\alpha_n \sigma^2}{|h_n^{OMA}|^2} \tag{5.31}$$

where N is the number of users, R_{min} is the required minimum rate for each user, $|h_n^{OMA}|^2$is the n^{th}users's channel gain in OMA scheme, $\alpha_n = 1/N$ is the allocated part of physical resources for the n^{th}user in OMA scheme where $n \in \{1, \dots, N\}$, and σ^2 is the noise power. Thus, the maximum power value P_{max} is determined as follows:

$$P_{max} = \max_{n \in \{1,\dots,N\}} \{p_{n,min}^{OMA}\} \tag{5.32}$$

where N is the number of users, and $p_{n,min}^{OMA}$ is the required minimum transmitted power for the n^{th}user in OMA scheme given in (5.31).

Assuming that all users of the OMA system transmit at the maximum power P_{max} given in (5.32), then the transmission rate $R_n^{OMA}$for the user n becomes as follows:

$$R_n^{OMA} = \alpha_n log2(1 + \frac{P_{max} |h_n^{OMA}|^2}{\alpha_n \sigma^2}) \tag{5.33}$$

where $p_{n,min}^{OMA}$ is the maximum transmitted power given in (5.32), $|h_n^{OMA}|^2$ is the n^{th}users's channel gain in OMA scheme, $\alpha_n = 1/N$ is the allocated part of physical resources for the n^{th}user in OMA scheme where $n \in \{1, \dots, N\}$, and σ^2 is the noise power. So the ε value can be specified as follows:

$$\varepsilon = \left| max\, \{R_n^{OMA}\}_{n=1}^{N} - min\, \{R_n^{OMA}\}_{n=1}^{N} \right| \tag{5.34}$$

where R_n^{OMA} is the rate for the n^{th}user in the OMA scheme given in (5.33). Since all OMA users are transmitting at the maximum power P_{max}, the total power is given by the following formula:

$$P_{total}^{OMA} = \sum_{n=1}^{N} P_{max} = NP_{max} \quad (5.35)$$

While the total power in the hybrid NOMA system depends on the values of the power $P = [p_1, \dots, \mathrm{p}_n, \dots, \mathrm{p}_N]$ allocated in the system and resulting from solving the problem (P1) and written as follows:

$$P_{total} = \sum_{n=1}^{N} p_n \quad (5.36)$$

Comparing the equations (5.35) and (5.36) and relying on the fact that the allocated powers are limited by the maximum power P_{max} (i.e. $P_n \leq P_{max}, \forall n \in \{1, \dots, N\}$), the total power in the NOMA scheme is equal or less than the total power in the OMA scheme ($P_{total} \leq P_{total}^{OMA}$). The powers shown in (5.35) and (5.36) are normalized to the noise power σ^2 for comparison to become the total power to noise power ratio equal to P_{total}^{OMA}/σ^2 for the OMA benchmark, and P_{total}/σ^2 for the NOMA scheme.

6. RESULTS AND DISCUSSION

The MATLAB environment is used to derive conclusions and evaluate the performance of the proposed scheme. The complex spreading sequences shown in Figure 6.1 are selected, which are composed of the complex elements given in Figure 4.2a. Complex spreading sequences can be generated randomly with a number that matches the number of users and the length $\boldsymbol{L}$ of each sequence. But twenty complex spreading sequences of length $\mathrm{L} = 4$ were selected to run the simulation at a specific set of sequences. So that the matrix of spreading sequences is partially selected from the matrix shown in Figure 6.1 according to the required number of users. The user overload in this case can reach 500% according to the simulation parameters shown in Table 6.1. Supposing that the Rayleigh flat fading channel is applied in our system model and the channel coefficients are known at both transmitter and receiver.

$$\begin{bmatrix} -1+1i, & -1+1i, & +1-1i, & -1-1i, & +1-1i, & +1-1i, & -1+1i, & +1+1i, & -1-1i, & +1+1i, & -1-1i, & +1-1i, & +1+1i, & +1+1i, & -1-1i, & -1+1i, & -1+1i, & -1-1i, & -1+1i, & -1+1i \\ -1+1i, & -1-1i, & +1+1i, & +1+1i, & +1-1i, & -1+1i, & -1+1i, & -1-1i, & +1+1i, & +1-1i, & -1+1i, & -1+1i, & -1-1i, & -1+1i, & -1-1i, & +1+1i, & -1+1i, & -1+1i, & +1+1i, & +1-1i \\ -1-1i, & -1-1i, & -1+1i, & -1+1i, & -1+1i, & +1-1i, & -1-1i, & -1+1i, & +1+1i, & -1-1i, & -1-1i, & +1-1i, & -1-1i, & +1+1i, & +1-1i, & -1+1i, & +1+1i, & +1+1i, & +1-1i, & -1+1i \\ -1+1i, & -1+1i, & +1-1i, & +1-1i, & +1+1i, & -1-1i, & +1-1i, & -1-1i, & -1-1i, & -1-1i, & +1-1i, & +1-1i, & +1+1i, & -1+1i, & +1-1i, & -1-1i, & -1+1i, & +1-1i, & +1-1i, & +1+1i \end{bmatrix}$$

Figure 6.1 Complex spreading sequences matrix

Table 6.1 Simulation coefficients

DESCRIPTION	SYMBLE	VALUES
Length of complex spreading sequence	L	4
Number of users	N	$L: L/2: 5L$
Noise power (dBm)	σ^2	-114
Maximum number of iterations for Algorithm2 and Algorithm3	t_1, t_2	$1, 2, 3, \dots, 20$
Required minimum rate values (b/s/Hz)	R_{min}	$0.01: 0.01: 2$
Number of transmitted symbol	N_d	1000

The extracted results represent the performance of the OMA benchmark system as well as the evaluation of the performance of the hybrid NOMA system for the following four conditions:

First case: System simulation for the matrix of the original spreading sequences partially selected from the matrix shown in Figure 6.1, so that all users transmits with the maximum available power p_{max} calculated by Equation (5.32).

Second case: System simulation for the matrix of spreading sequences generated by applying Alogrithm2 presented in Table 5.2 , so that all users transmits with the maximum available power p_{max} calculated by the Equation (5.32).

Third case: System simulation for the original matrix of spreading sequences partially selected from the matrix shown in Figure 6.1, so that users transmits with the powers results from Alogrithm3 implementation shown in Table 5.3.

Fourth case: System simulation for the matrix of spreading sequences generated by applying Alogrithm2 shown in Table 5.2, so that users transmits with the powers results from Alogrithm3 implementation shown in Table 5.3.

The results are extracted as an average of applying the previously described algorithms at one transmitted symbol from each user and iterate $N_d = 1000$ times. In each time, different AWGN samples are generated with fixed power σ^2 and different channel coefficients with flat fading .

6.1 Achievable Minimum Rate Performance

Achievable minimum rates for the earlier mentioned four cases and in the OMA benchmark are incremented, when the required minimum rate is grown, as shown in Figure 6.2, where the number of users $N = 6$ and the maximum number of iterations for Algorithm2 and Algorithm3 $t_1 = t_2 = 10$. But this increase becomes very small in the first and second cases compared to the third and fourth cases and even in the OMA benchmark. The achievable minimum rate is equal to the required minimum rate in the OMA benchmark. This because the scheme was designed based on setting the maximum available power that achieves the required rate. It is noted that the hybrid NOMA scheme in its four cases achieves an achievable minimum rate better than the OMA benchmark. The results of Figure 6.2 show that the hybrid NOMA scheme in the fourth case outperforms the rest in terms of an achievable minimum rate, where in the fourth case an achievable minimum rate is equal to 6.53b/s/Hz at $R_{min} = 1\text{b/s/Hz}$, which means an increment of 5.53b/s/Hz compared to the OMA benchmark (gain is 653%). While in the third case a gain of 614% can be achieved, in the second of 419% and the first of 318%, compared to the OMA benchmark at the same the required minimum rate $R_{min} = 1\text{b/s/Hz}$.

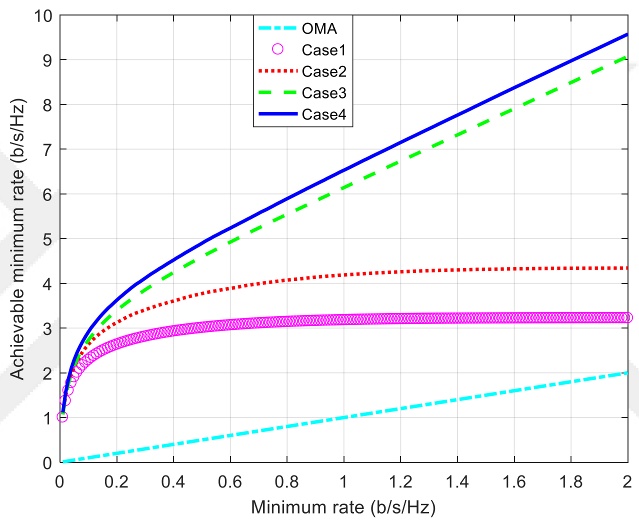

Figure 6.2 Achievable minimum rate at various required minimum rate values for N=6 and $t_1 = t_2 = 10$.

The performance improvement shown in Fig. 6.2 for the third and fourth cases is due to raising the minimum SINR and reducing the difference between the maximum and minimum rates according to constraint (5.20c) in problem (P1). This results corresponds to an increase in the achievable minimum rate although the rate decreased for some users, as shown in Figure 6.3, which is a sample view of the transmission rate for each user. In the OMA benchmark, the difference between the maximum and minimum rate is $\varepsilon = 1.559 - 1 = 0.559\text{b/s/Hz}$, while in the third and fourth cases $\varepsilon_3 = 6.254 - 5.915 = 0.339\text{b/s/Hz} < \varepsilon$, $\varepsilon_4 = 6.286 - 5.991 = 0.295\text{b/s/Hz} < \varepsilon$,respectively. In the first case $\varepsilon_1 = 10.94 - 2.342 = 8.598\text{b/s/Hz} > \varepsilon$ and in the second case $\varepsilon_2 = 11.08 - 3.349 = 7.731\text{b/s/Hz} > \varepsilon$.

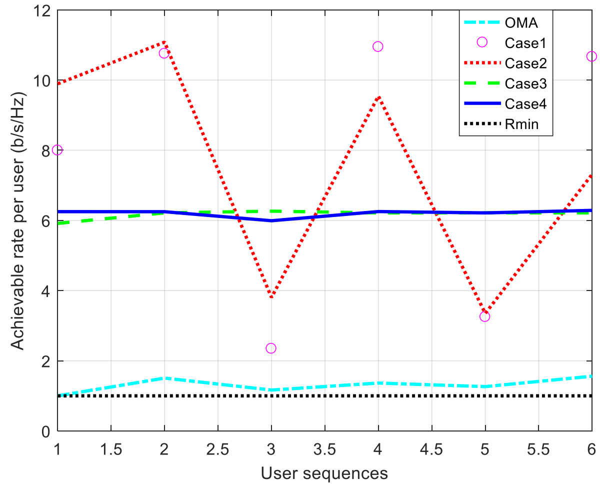

Figure 6.3 Samples of achievable minimum rate for 6 users where R_{min}=1b/s/Hz and t_1= t_2 =10.

Figure 6.4 shows the powers allocated to each user in the four cases of the hybrid NOMA scheme and in the OMA benchmark, which correspond to the results shown in Figure 6.3, where the maximum power calculated in (5.32), $N = 6$, $R_{min} = 1b/s/Hz$, and$t_1 = t_2 = 10$. The transmission powers of users vary in the third and fourth cases, as shown in Figure 6.4. While, all users transmit with the maximum power in the rest of the schemes. For example, the second user transmits with a power of -104.7dBm in the fourth case and -103.9dBm in the third case and achieves a rate higher than required minimum rate, while it transmits with a power of -90.14dBm higher than in the first and second cases. But its transmission rate is higher than the one of third and fourth cases, as shown in Figure 6.3.

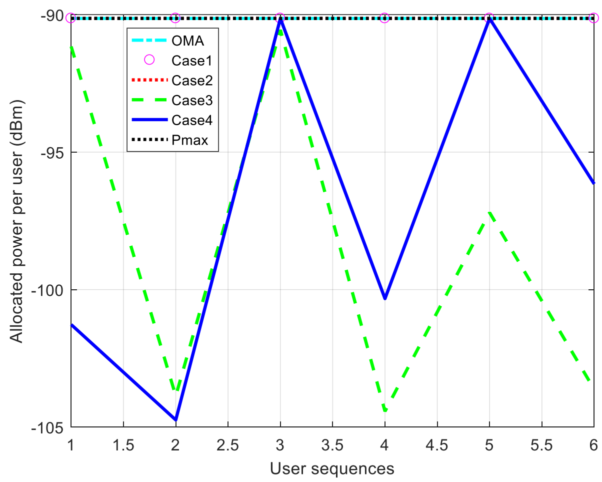

Figure 6.4 Samples of allocated powers for 6 users where R_{min}=1b/s/Hz and t_1= t_2 =10.

The performance of the Achievable minimum rate is improved by increasing the maximum number of iterations t_1, t_2, as shown in Fig. 6.5 where $N = 6$ and $R_{min} = 1b/s/Hz$ for the second, third and fourth cases that depend on the use of iterative algorithms: Algorithm2 and Algorithm3. But the increase in the maximum number of iterations means an increase in the complexity of the system. However, it is noted from Figure 6.5 that the hybrid NOMA scheme in the first case achieves a fixed gain of 318.6% compared to the OMA benchmark. While, the hybrid NOMA scheme in the second, third and fourth cases achieve gains of 356.9% , 483.3% and 518.2% , respectively, for one iteration $t_1 = t_2 = 1$.

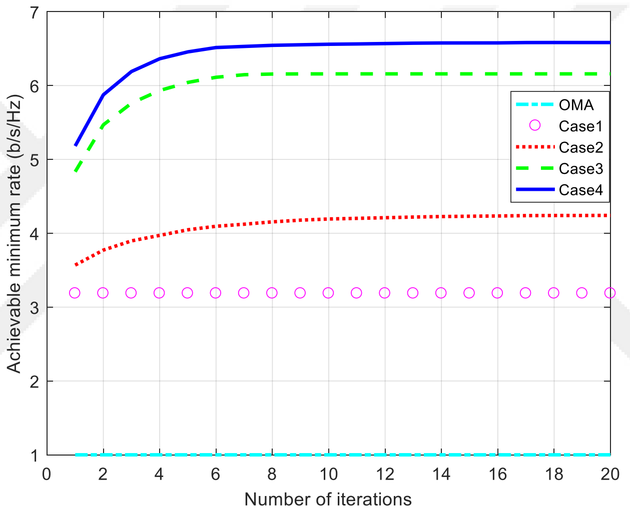

Figure 6.5 Achievable minimum rate at various numbers of iterations where N=6 and R_{min}=1b/s/Hz.

The performance of the hybrid NOMA scheme is affected by increasing UOL in terms of achievable minimum rate. When, the number of users increases, the achievable minimum rate decreases in the four cases, as shown in Figure 6.6, where $R_{min} = 1b/s/Hz$ and $t_1 = t_2 = 10$. The hybrid NOMA scheme in the third and fourth cases performs better than in the first and second cases as the performance collapses faster in these two cases to the point that the required minimum rate is not able to be met. For useroverloading = 400% (corresponding to the number of users $N = 16$) and $R_{min} = 1b/s/Hz$, it is found the achievable minimum rate less than $0.9b/s/Hz$ in the first and second cases. While, it exceeds $2b/s/Hz$ in the third and fourth cases. The transmission powers in the OMA benchmark are set such that the required minimum rate is met for each user so that the minimum rate does not change with an increase in the number of users in this scheme, as shown in Figure 6.6.

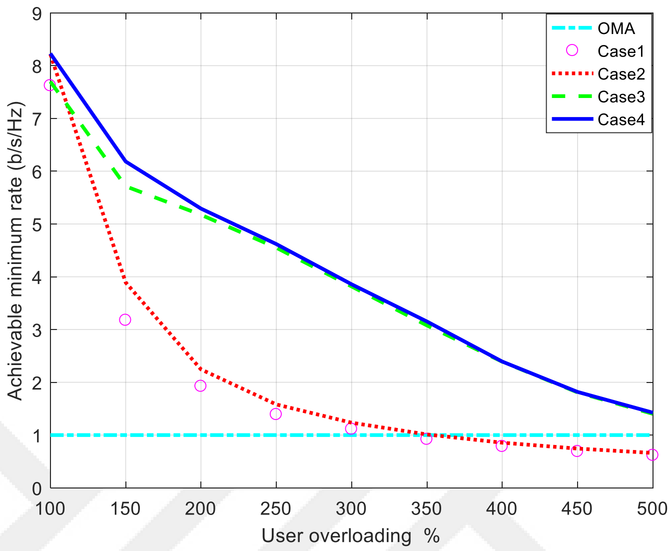

Figure 6.6 Achievable minimum rate at various UOL values where R_{min}=1b/s/Hz and t_1= t_2 =10.

The simulation results in Figures 6.2 through 6.6 show the effectiveness of the proposed algorithms to improve the performance in terms of minimum rate with different percentages and the possibility of raising achievable minimum rate with different percentages up to more than 500% in some cases.

6.2 Total Power to Noise Power Ratio Performance

The effectiveness of the proposed algorithms in the hybrid NOMA scheme is not limited to improving the performance of the minimum rate. But it also contributes to reducing the total power consumed in the system, as shown in Figure 6.7, where the maximum power P_{max} and the total power to noise power ratio increases with the increasing required minimum rate. For $R_{min} = 1b/s/Hz$, $t_1 = t_2 = 10$ and $N = 6$. The total power to noise power ratio is equal to 39.88dB in the OMA benchmark and the first and second cases. While, it becomes 34.67dB and 35.39dB in the third and fourth cases, respectively. i.e it is possible to save 65% from the total power consumed at these values.

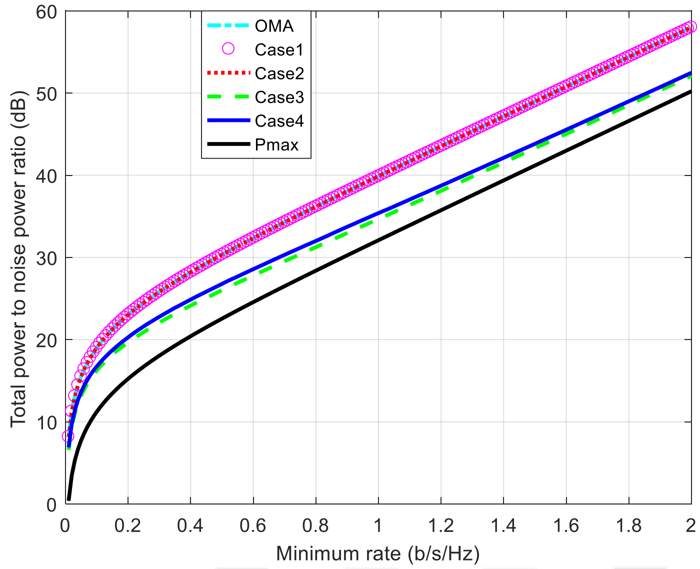

Figure 6.7 Total power to noise power ratio at required minimum rate values where N=6 $t_1 = t_2 = 10$..

The total power to noise power ratio is affected by the maximum number of iterations t_1, t_2 in the third and fourth cases to become almost constant after the sixth iteration, as shown in Figure 6.8 where $R_{min} = 1b/s/Hz$ and $N = 6$. So for $t_1 = t_2 = 6$, the total power to noise power ratio in the third case is 37.77dB, and in the fourth case is 37.86dB, which is equivalent to saving the total power by $\approx 33\%$ for the third case and $\approx 25\%$ for the fourth case compared to the total power consumed at $t_1 = t_2 = 1$. From Figure 6.8, it is noticed that the performance of the second case is constant with the maximum number of iterations, despite the use of the second iterative algorithm. This is because the power allocated to all users is maximum P_{max}in this case, and this also applies to the first case and the OMA benchmark.

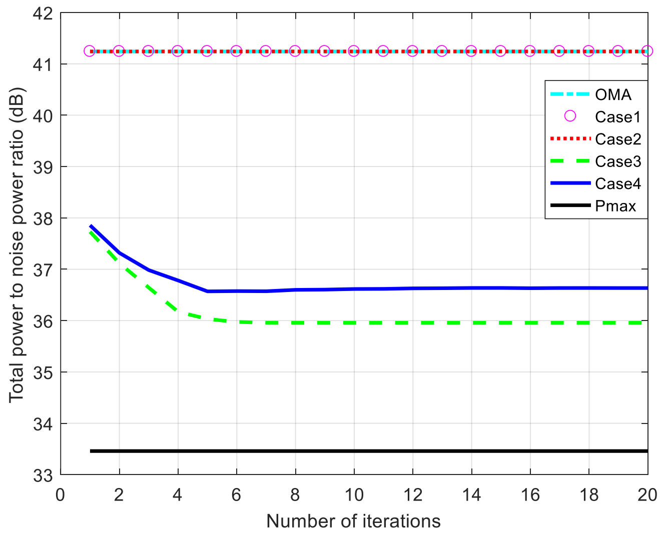

Figure 6.8 Total power to noise power ratio at various numbers of iterations where N=6 and R_min=1b/s/Hz

It is normal for the total power to noise power ratio to increase as the UOL increases as shown in Figure 6.9, where $R_{min} = 1b/s/Hz$ and $t_1 = t_2 = 10$. This is because of the increase in the number of transmitting devices. But this percentage of the third and fourth is lower than the one of other cases and the OMA benchmark. For example, when useroverloading = 400%, it can be saved 60% from the consumed power where the total power to noise power ratio is (77.32dB) in the third and fourth cases and (81.28dB) in the rest of the schemes.

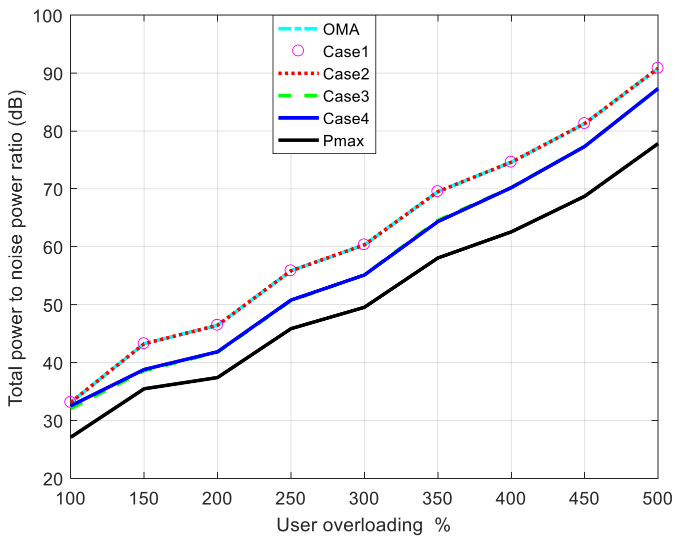

Figure 6.9 Total power to noise power ratio at various UOL values where R_{min}=1b/s/Hz and t_1= t_2 =10.

The simulation results in this section show the superiority of the proposed algorithms to provide the total power consumption of the hybrid NOMA system compared to the OMA benchmark and even the conventional hybrid NOMA system.

6.3 Error Probability Performance

The proposed algorithms for the hybrid NOMA system model helps to reduce the BER, as shown in Figure 6.10, where $t_1 = t_2 = 10$ and $N = 6$. The theoretical error probability in the third and fourth cases is lesser than 10^{-6} at $R_{min} = 1b/s/Hz$, while in the first is $\sim 10^{-3}$and in the second is $\sim 10^{-5}$. It can be seen from Figure 6.10 that the error probability decreases as the required minimum rate increases due to the increasing in the minimum signal to interference and noise ratio which is the main objective of the problem (P1) and it is the same reason that raises the minimum rate, as shown in Figure 6.2.

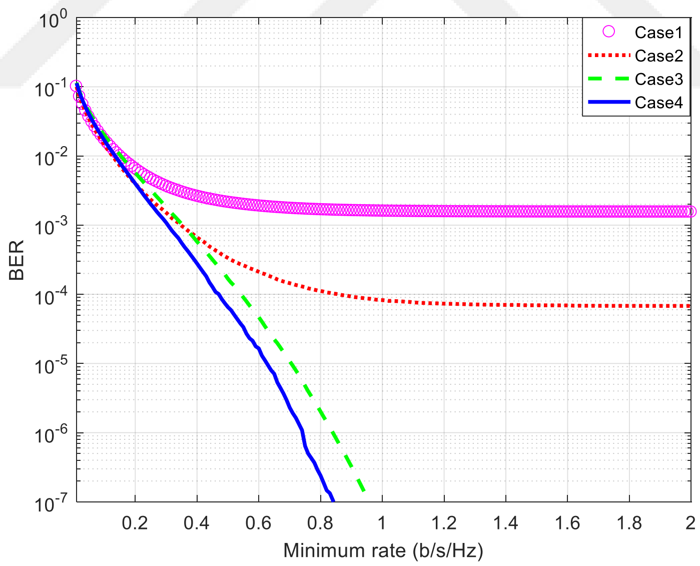

Figure 6.10 BER at required minimum rate values where N=6 and t_1= t_2 =10.

In addition, the BER in the system decreases as the total power to noise power ratio increases, as shown in Fig. 6.11 where $t_1 = t_2 = 10$and $N = 6$. But the performance of the error probability is improved in the third and fourth cases than it was in the first and even the second cases. When the total power to noise power ratio is 25dB, the error is

$BER = \sim 10^{-3}$in the first and second cases. While, it improves in the remaining two cases to become $BER = \sim 10^{-4}$.

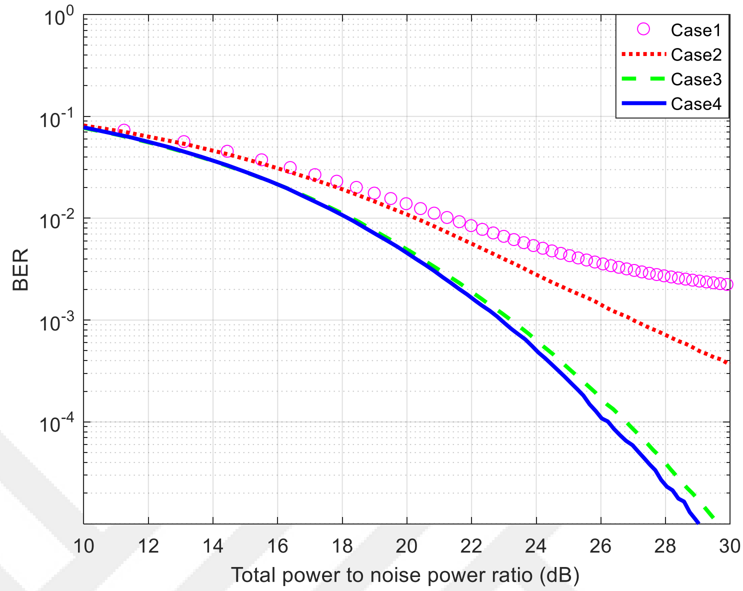

Figure 6.11 BER versus total power to noise power ratios where N=6 and $t_1 = t_2 = 10$.

The error probability decreases with increasing maximum number of iterations, as shown in Fig. 6.12, where $R_{min} = 1b/s/Hz$ and $N = 6$. But the best performance is in the fourth case. The performance becomes almost constant after the sixth iteration in the second and third cases, but the error probability becomes a hundred times lesser, when the number of iterations increases from 1 to more than 6 in the third and fourth cases. For the comparison at $t_1 = t_2 = 1$ between the four cases, it is noticed that the error probability decreases by a small amount in the second case compared with the first case. While, it is a hundred times lesser in the third and fourth cases than it was in the first case.

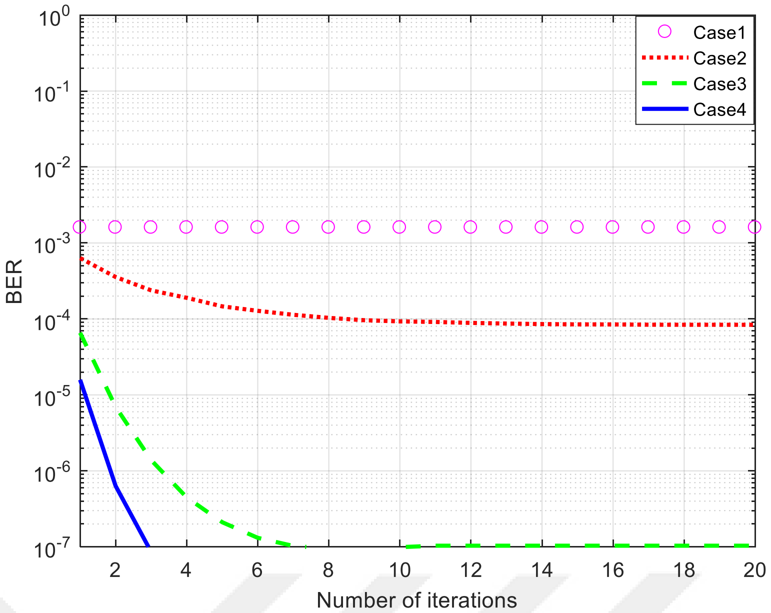

Figure 6.12 BER at various numbers of iterations where N=6 and R_{min}=1b/s/Hz

The effect of high UOL on BER performance is shown in Figure 6.13, where the error probability increases with increasing UOL for $R_{min} = 1b/s/Hz$ and $t_1 = t_2 = 10$. However, the proposed iterative algorithms in the third and fourth cases contributed to reduce the error probability especially when UOL > 100%. For example, when UOL = 400%, the system BER becomes $BER_{3,4} = 2.5 \times 10^{-3}$ instead of $BER_{1,2} = 6.5 \times 10^{-2}$ in the first and second cases. But when UOL = 200%, the error probability decreased by a thousand times compared to the first and second cases.

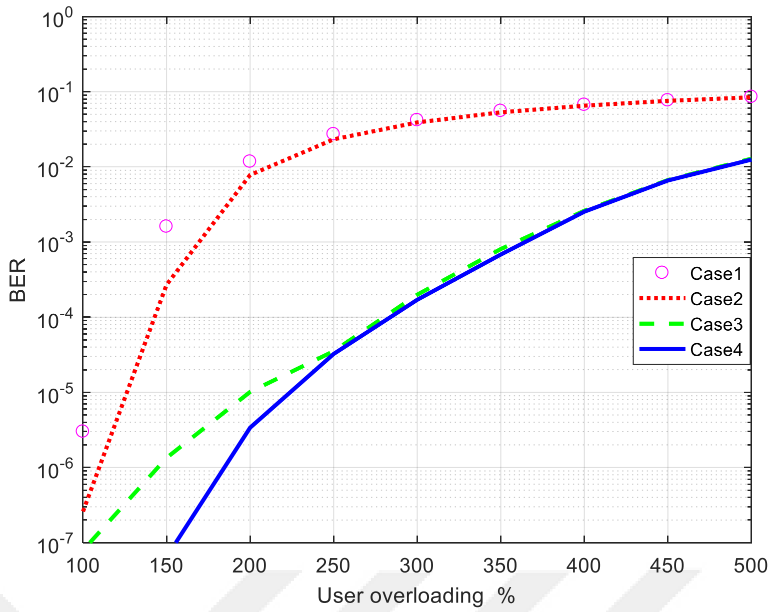

Figure 6.13 BER at various UOL values where R_{min}=1b/s/Hz and t_1= t_2 =10.

The proposed scheme for the hybrid NOMA system contributed to improve the BER performance of the system compared to the traditional system as indicated by the results in this section, and this would preserve the advantages gained from the system in terms of transmission rates. The scheme is acheived 4dB gain in power compared to the scheme existing in (Ameur 2020) at BER=10^{-2} , where the total power to noise power ratio in proposed scheme is 18dB and in (Ameur 2020) is 22dB. That comparison was made for Figure (6.11) in our thesis and Figure 2. in (Ameur 2020) where UOL=150% (N=6). On the other hand, the BER performance of the proposed scheme is better than existing in (Ameur 2020) as shown in Table 6.2 at any the total power to noise power ratios.

Table 6.2 Numerical comparison between the proposed scheme and the scheme existing in (Ameur 2020)

TOTAL POWER TO NOISE POWER RATIO (dB) / **BER**		18	20	22	25
BER in proposed scheme	0.03	0.01	0.005	0.002	0.0002
BER in (Ameur 2020)	0.15	0.06	0.03	0.01	0.001

7. CONCLUSIONS AND RECOMMENDATION

In this project, it was introduced the main concept and advantage of NOMA techniques, which were considered as one of the promising solutions to address the emergency challenges in 5G system and beyond. The main focus was on multi-user sharing access and the power domain NOMA schemes, which are types of NOMA technologies that improved system throughput, increased the number of users on the same radio resource. Both PD-NOMA and MUSA schemes was used in both downlink and uplink system based on MMSE-SIC receiver to improve decoding performance. In general, the performances of NOMA methods such bit rate, fairness, and error probability were depended on the signal to interference and noise ratio. They were related to the auto and cross correlation characteristics of complex spreading sequences in MUSA scheme and power allocation in PD NOMA.

The algorithm was proposed to maximize the minimum signal to interference and noise ratio in hybrid NOMA uplink including the MUSA and PD NOMA, under the required minimum rat, fairness, and maximum transmitted power constraints. The non convex formulated proplem was divided into two sub problems to find near optimum spreading sequences and power allocation separately, based on two iterative algorithms. In the first iterative algorithm, the optimum complex spreading sequences allocation was determined under the assumption that each user transmits with maximum allowed power, then the optimum power allocation was found by using the second iterative algorithm. Besides, OMA scheme was proposed as a benchmark and to find the maximum power corresponding to the required minimum rate. The simulation results were indicated that our proposed scheme outperforms on the OMA benchmark in terms of achievable minimum rate per user and total power consumption. Also, the results show that the BER performance was improved in the proposed scheme compared to the conventional MUSA scheme.

The impact of imperfect successive interference cancellation was ignored, which was the practical case. So, it was interested to reformulate and solve the main problem under this consideration. Also, the effect of channel estimation error was left as a future study.

According to the distinction performance of hybrid NOMA schemes, it was investigated using SCMA for the enhancement of uplink performance.

REFERENCES

Akbar, A. J. 2021. NOMA and 5G emerging technologies: A survey on issues and solution techniques. Computer Networks 190 .

Alghasmari, W.F. 2021. Optimal Power Allocation in Downlink Non-Orthogonal Multiple Access (NOMA). International Journal of Advanced Computer Science and Applications (IJACSA) (12), 318 – 325.

Ali, S. 2016. Non-orthogonal multiple access (NOMA) for downlink multiuser MIMO systems: User clustering, beamforming, and power allocation. IEEE access (5), 565–577.

Alsabah, M.N. 2021. 6G wireless communications networks: a comprehensive survey. IEEE Access.

Ameur, W.B. 2020. Power allocation for BER minimization in an uplink MUSA scenario. 2020 IEEE 91st Vehicular Technology Conference (VTC2020-Spring). Antwerp, Belgium.

Ameur, W. M. 2021. Autonomous power decision for grant free access MUSA scheme in mMTC scenario. Retrieved from https://hal.archives-ouvertes.fr/hal-03101354

Bhatia, R. 2018. Multiple access techniques for 5G networks. International Journal of Engineering Technologies and Management Research (5), 305-314.

Budhiraja, I.E. 2021. A Systematic Review on NOMA Variants for 5G and Beyond. IEEE Access (9), 85573-85644.

Cui, J.D. 2016. A Novel Power Allocation Scheme Under Outage Constraints in NOMA Systems. IEEE Signal Processing Letters (23), 1226 – 1230.

Dai, L.E. 2018. A Survey of Non-Orthogonal Multiple Access for 5G. IEEE Communication Surveys & Tutorials (20), 2294–2323.

Eid, M. F. 2019. Performance analysis of 5-ary MUSA and SCMA for uplink transmission. Indonesian Journal of Electrical Engineering and Computer Science (15), 365-372.

Evren, Ç. F. 2019. Multi-user shared access in massive machine-type communication systems via superimposed waveforms. ELSEVIER journal, Physical Communication (37).

Goldsmith, A. 2005. In Wireless Communication. Cambridge University Press.

Hayat, O. N. 2021. Springer. Retrieved from Multi-user Shared Access (MUSA) procedure for device discovery in D2D communication

Higuchi, K. a. 2015. Non-orthogonal Multiple Access(NOMA) With Successive Interference Cancellation for Future Radio Access. IEICE Transactions on Communications (E98-B), 403-414.

id, M. F. 2017. Performance Analysis of MUSA with different Spreading Codes Using Ordered SIC Methods. 12th International Conference on Computer Engineering and Systems.

Islam, M. R. 2017. Power domain non-orthogonal multiple access (NOMA) in 5G systems: Potentials and challenges. IEEE Communication Surveys & Tutorials (19), 721–742.

Jha, M.K. 2021. NOMA MIMO Visible Light Communication with ZF-SIC and MMSE-SIC. 2nd PhD Colloquium on Ethically Driven Innovation and Technology for Society (PhD EDITS). Banglore,India: IEEE.

Lian, L. A. 2021. Multiple Access Technologies for 5G. Berlin/Munich/Boston: De Gruyter.

Liu, L.E. 2018. Sparse Signal Processing for Grant-Free Massive Connectivity. IEEE Signal Processing Magazine , 88-99.

Liu, Y. E. 2017. Non-orthogonal Multiple Access for 5G and Beyond. Non-orthogonal Multiple Access for 5G and Beyond. Proceedings of the IEEE, (105), 2347-2381.

Meng, X. W. 2018. Turbo-like Iterative Multi-user Receiver Design for 5G Non-orthogonal Multiple Access. IEEE 88th Vehicular Technology Conference.

Okamoto, E.M. 2019. Performance Comparison of Multi-User Shared Multiple Access Scheme in Uplink Channels. IEICE TRANS. COMMUN. (E102–B), 1458-1466.

Paudel, P. 2018. 5G Telecommunication Technology: History, Overview, Requirements and Use Case Scenario in Context of Nepal. . In C. IT4D (Ed.).

Saito, Y. e. 2013. Non-orthogonal multiple access (NOMA) for cellular future radio access. IEEE 77th vehicular technology conference (VTC Spring), (pp. 1–5).

Salih, A. A. 2020. Evolution of Mobile Wireless Communication to 5G Revolution. Kansai University.

Sari, H. 2000. Extending the Capacity of Multiple Access Channels . IEEE Communications Magazine , 74-82.

Shah, S. E. 2021. Survey and Performance Evaluation of Multiple Access Schemes for Next-Generation Wireless Communication Systems. IEEE (9).

Shan, Y. P. 2017. Uplink Multiple Access Schemes for 5G: A Survey. ZTE COMMUNICATIONS (15), 31-40.

Sharma 2018. Joint Power-domain and SCMA-based NOMA System for Downlink in 5G and Beyond . IEEE Communications Letters.

Shengli, Z.A. 2003. Adaptive modulation for multiantenna transmissions with channel mean feedback. IEEE International Conference on Communications, (pp. 2281–2285).

Sousa, M. V. 2018. A Survey on the 5th Generation of Mobile Communications. ISEL Academic Journal of Electronics Telecommunications and Computers (4).

TATARIA, H. 2021. 6G Wireless Systems: Vision, Requirements, Challenges, Insights, and Opportunities. IEEE (109).

Vaezi, M. O. 2018. Multiple Access Techniques for 5G Wireless Networks and Beyond. Springer. Switzerland: Springer.

Yang, Z. D. 2017. The impact of power allocation on cooperative non-orthogonal multiple access with SWIPT. Transactions on wireless communications (6).

Yuan, Z. E. 2016. Multi-User Shared Access for IoT. IEEE 83rd Vehicular Technology Conference (VTC Spring).

Zhai, D. Z. 2018. Energy-Efficient User Scheduling and Power Allocation for NOMA-Based Wireless Networks With Massive IoT Devices. IEEE Internet of Things Journal (5), 1857 – 1867.

CURRICULUM VITAE

Personal Information

Name and Surname : Wael Sadeq Abd Ali FANHARAWY

Education

MSc	Çankırı Karatekin University Graduate School of Natural and Applied Sciences Department of Electrical and Electronis Engineering	2020-2023
Undergraduate	Çankırı Karatekin University Faculty of Engineering Department of Electrical and Electronis Engineering	2009-2012

Academic Activities

1. W.S.A.A. Fanharawy, M. Ari, and M.E. Yigit. 2023. Investigating the role of multi-user access in 5G network. Technical and Physical Problems of Engineering, 56(15).